iScience

CellPress
OPEN ACCESS

Article

Transgenesis of mammalian PABP reveals mRNA polyadenylation as a general stress response mechanism in bacteria

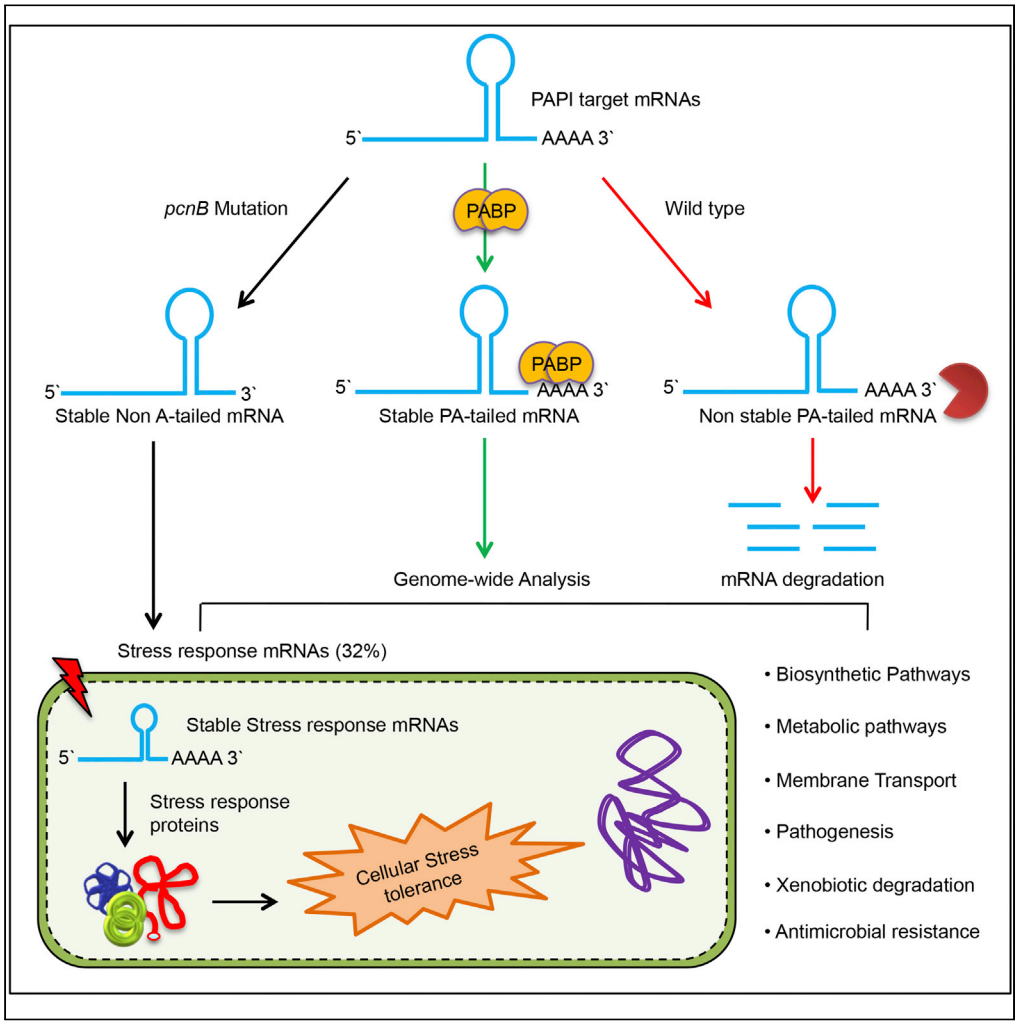

Nimmy Francis, Rakesh S. Laishram

laishram@rgcb.res.in

Highlights

Trans expression of mammalian PABPN1 stabilizes polyadenyated mRNAs in *E. coli*

PABPN1 expression phenocopies *pcnB* mutation and regulates plasmid copy number

3′-polyadenylation acts as a general stress response mechanism in bacteria

This study indicates an evolutionary significance of PABP in mRNA metabolism

Francis & Laishram, iScience *24*, 103119
October 22, 2021 © 2021
https://doi.org/10.1016/j.isci.2021.103119

iScience

CellPress
OPEN ACCESS

Article

Transgenesis of mammalian PABP reveals mRNA polyadenylation as a general stress response mechanism in bacteria

Nimmy Francis[1,2] and Rakesh S. Laishram[1,3,*]

SUMMARY

In eukaryotes, mRNA 3′-polyadenylation triggers poly(A) binding protein (PABP) recruitment and stabilization. In a stark contrast, polyadenylation marks mRNAs for degradation in bacteria. To study this difference, we trans-express the mammalian nuclear PABPN1 chromosomally and extra-chromosomally in *Escherichia coli*. Expression of PABPN1 but not the mutant PABPN1 stabilizes polyadenylated mRNAs and improves their half-lives. In the presence of PABPN1, 3′-exonuclease PNPase is not detected on PA-tailed mRNAs compromising the degradation. We show that PABPN1 trans-expression phenocopies *pcnB* (that encodes poly(A) polymerase, PAPI) mutation and regulates plasmid copy number. Genome-wide RNA-seq analysis shows a general up-regulation of polyadenylated mRNAs on PABPN1 expression, the largest subset of which are those involved in general stress response. However, major global stress regulators are unaffected on PABPN1 expression. Concomitantly, PABPN1 expression or *pcnB* mutation imparts cellular tolerance to multiple stresses. This study establishes mRNA 3′-polyadenylation as a general stress response mechanism in *E. coli*.

INTRODUCTION

Polyadenylation (addition of a poly-adenosine tail, PA-tail) by poly(A) polymerase (PAP) enzymes at the 3′-end is a key-processing event of nascent transcripts that determines fate of a cellular messenger RNA (mRNA) (Bardwell et al., 1990; Dreyfus and Regnier, 2002; Shatkin and Manley, 2000; Zheng and Tian, 2014). In mammals, almost all mRNAs are polyadenylated (~250 adenosines) inside the nucleus, which are subsequently shortened (~70–100 adenosines) after cytoplasmic processing (Eckmann et al., 2011; Jalkanen et al., 2014; Laishram, 2014). PA-tail endows stability to the mRNA and is required for efficient translation (Glaunsinger and Lee, 2010; Laishram, 2014). On the contrary, PA-tail addition marks mRNAs for degradation in prokaryotes (Belasco, 2010; Hajnsdorf et al., 1995; Hajnsdorf and Regnier, 1999; Sarkar, 1997). Also, PA-tails are short (15–40 adenosines in *E. coli*) and are present on limited mRNAs (Sarkar, 1997). However, recent studies indicate widespread polyadenylation of bacterial transcripts including ribosomal RNAs, transfer RNAs, non-coding RNAs, small RNAs and mRNAs (Li et al., 1998; Maes et al., 2016; Mohanty et al., 2012; Reichenbach et al., 2008; Xu et al., 1993). Polyadenylated transcripts largely have structured 3′-ends, and that addition of a PA-tail provides platform for the 3′-exonuclease polynucleotide phosphorylase (PNPase) to initiate 3′–5′ exonucleolytic degradation along with other degradosome complex components [ribonuclease E (RNase E), RNA helicase B (RhlB) and enolase] (Blum et al., 1999; Carpousis, 2007). Thus, bacterial polyadenylation primarily regulate turnover and quality control of specific cellular transcripts (Mohanty and Kushner, 2011).

Poly(A) polymerase I (PAPI) encoded by *pcnB* gene is the primary PAP in *E. coli* (Liu and Parkinson, 1989; Xu et al., 1993), yet, *pcnB* gene is dispensable in the cell (Masters et al., 1993). On the other hand, PAPI overexpression exhibits cellular toxicity by rapid polyadenylation of tRNAs and inhibiting protein synthesis (Mohanty and Kushner, 2012). Therefore, PAPI level is maintained low *in vivo* via a non-canonical initiation codon and a poor ribosome binding site despite transcribing from multiple promoters (three σ70-and two σS-dependent promoters) (Binns and Masters, 2002; Jasiecki and Węgrzyn, 2006; Nadratowska-Wesołowska et al., 2010). PAPI is primarily known for the regulation of colE1-based plasmid replication by controlling *RNAI* transcript stability (He et al., 1993; Xu et al., 1993). Recent studies have now established role of PAPI-mediated polyadenylation in functional gene expression and have linked with stationary phase

[1]Cardiovascular and Diabetes Biology Group, Rajiv Gandhi Centre for Biotechnology, Thycaud Post, Poojappura, Trivandrum 695014, India

[2]Manipal Academy of Higher Education, Manipal 576104, India

[3]Lead contact

*Correspondence: laishram@rgcb.res.in

https://doi.org/10.1016/j.isci.2021.103119

growth, chemotaxis and motility, nutrient starvation, and envelop stress (Aiso et al., 2005; Carabetta et al., 2010; Joanny et al., 2007; Maes et al., 2013, 2016; Mohanty et al., 2012, 2020; Reichenbach et al., 2008; Sinha et al., 2018). However, the complete pool of polyadenylated mRNAs and a wide range of physiological processes regulated by general polyadenylation are yet to be determined.

Poly(A) binding proteins (PABPs) bind PA-tail and protects PA-tailed mRNAs from nuclease degradation in eukaryotes (Bernstein and Ross, 1989; Kuhn and Wahle, 2004). In mammals, there are three cytoplasmic PABPs (PABPC1, PABPC2, and PABPC3) and one nuclear PABP (PABPN1) (Kuhn and Wahle, 2004). While cytoplasmic PABP is critical for the stability and translation of the mRNA, nuclear PABPN1 primarily promotes stability to the PA-tailed mRNAs and regulates PA-tail length control and mRNA nuclear export (Lemay et al., 2010). Two point mutations in the RNA binding domain of PABPN1 (tyrosine 175 to alanine, Y175A and phenylalanine 215 to alanine, F215A) are shown to compromise PA-tail mRNA binding and PABPN1 function (Kerwitz et al., 2003; Kuhn et al., 2003). No counterparts of eukaryotic PABPN1 that protects and stabilizes cellular PA-tailed mRNAs are known in bacteria (Dreyfus and Regnier, 2002). Two RNA binding proteins Hfq and cold shock-like protein E (CspE) in *E. coli* are reported to bind PA-containing RNAs *in vitro* (Feng et al., 2001; Folichon et al., 2003). Hfq can also promote PA-tail elongation by PAPI (Hajnsdorf and Regnier, 2000; Mohanty et al., 2004). Nonetheless, both CspE and Hfq interact with multiple RNA sequences and their effect on the PA-tail stabilization *in vivo* is unclear (Hajnsdorf and Boni, 2012; Hajnsdorf and Regnier, 2000; Mohanty et al., 2004; Phadtare and Inouye, 1999). Therefore, cellular functions of CspE and Hfq on mRNA metabolism are different from that of eukaryotic PABP mediated mRNA stabilization.

To understand the difference in the cellular roles of polyadenylation on mRNA metabolism in bacteria and eukaryotes, we trans-express mammalian PABPN1 in *E. coli*. Expression of PABPN1 but not the mutant PABPN1 defective for PA-tail binding stabilizes earlier reported polyadenylated mRNAs in *E. coli*. Consistent mRNA stabilization was observed in *pcnB* mutation with no additional effect of PABPN1 expression suggesting that PABPN1 affects polyadenylated transcripts. PABPN1 trans-expression also phenocopies *pcnB* mutation and stabilizes *RNAI* transcript thereby reducing copy number of colE1-based plasmids. We demonstrate that PABPN1 trans-expression compromises PNPase association and degradation of polyadenylated mRNAs. Genome-wide RNA-Seq analysis shows up regulation of a large number of transcripts on PABPN1 expression in *E. coli*. Functional analysis of the up regulated mRNAs reveals involvement of polyadenylation in new cellular functions that include stress response, membrane transport, cellular metabolism, xenobiotic degradation, and pathogenesis. Among the upregulated mRNAs, the largest fraction (~33%) is involved in response to multiple stresses such as osmotic, oxidative, acid, DNA alkylation, heat and cold stresses but without affecting the expression of known stress response regulators. We demonstrate that *pcnB* mutation and introduction of PABPN1 but not the mutant PABPN1 (compromised for PA-tail binding) stimulates expression of stress response genes and imparts cellular tolerance to multiple stresses. Our study establishes 3′-end mRNA processing as a general stress response mechanism in bacteria.

RESULTS

Trans-expression of mammalian nuclear poly(A) binding protein, PABPN1 in *E. coli*

In eukaryotes, PABP binding primarily protects PA-tails at the mRNA 3′-end and stabilizes polyadenylated mRNAs. Therefore, to assess the effect of PABP on mRNA turnover in bacteria, we trans-expressed mammalian nuclear PABPN1 in *E. coli* K-12 strain MG1655 and its isogenic *pcnB* mutant strain (Figure 1A, Table 1). PABPN1 was expressed first through pBAD18 plasmid and PABPN1 expression was tested by Western blot analysis using PABPN1-specific antibody. We observed PABPN1 expression in the pBAD18-*PABP* transformed cells but not in the plasmid control pBAD18 transformed cells after arabinose induction (Figure 1B). Near similar PABPN1 expression was observed in all media after induction with 0.5% arabinose (LB, Minimal-Glucose, or Minimal-Glycerol) in strains transformed with pBAD18-*PABP* but not in pBAD18 plasmid (Figure S1A). In a second approach, we expressed PABPN1 stably through chromosomal insertion using *λ-Inch* technique (Boyd et al., 2000) to obtain a stable single copy expression (Figure 1A). We confirmed PABPN1 integration into the genomic DNA by PCR analysis and expression by Western blot analysis in both wild type and *pcnB* mutant cells (Figures 1C and S1B). Hereafter, stable PABPN1 expressing cells are referred to as MG-*PABP* or *pcnB-PABP* respectively in the text. We observed similar results from both plasmid-based PABPN1 expression and chromosomal PABPN1 expression.

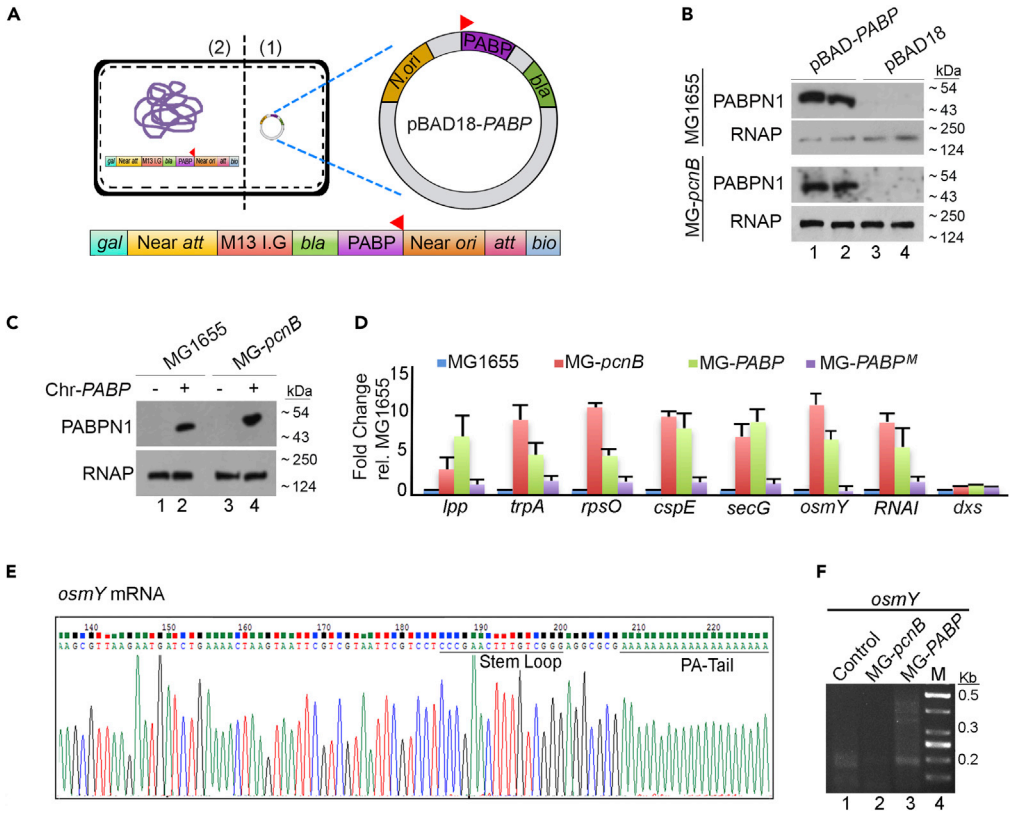

Figure 1. *Trans* mammalian nuclear PABPN1 expression stabilizes polyadenylated mRNAs in *E. coli*

(A) Schematic diagram of mammalian PABPN1 transgenesis in *E. coli*. (1) pBAD18 plasmid-based expression and (2) PABPN1 expression through chromosomal insertion by *λ-Inch* technology using pBAD18-*PABP* construct. PABPN1 insertion at the *att* sites in the inter-genic region between *gal* and *bio* operon is indicated.

(B) Western blot analysis of expressed PABPN1 and loading control RNA polymerase (RNAP) from MG1655 and *pcnB* mutant cells (MG-*pcnB*) transformed with pBAD18 or pBAD18-*PABP* plasmids in the presence of induction with 0.5% arabinose in LB-media.

(C) Western blot analysis of stable PABPN1 expression or loading control RNAP from MG1655 and isogenic *pcnB* mutant strain (MG-*pcnB*) with and without chromosomal PABPN1 insertion using specific antibodies as indicated.

(D and E) (D) qRT-PCR analysis of known polyadenylated mRNAs from wild type MG1655, PABPN1 (MG-*PABP*) or PABPN1 mutant (Y175A) (MG-$PABP^{M}$) expressed, and *pcnB* mutant (MG-*pcnB*) cells as indicated (p values, *lpp* < 0.001, *trpA* < 0.002, *rpsO* < 0.01, *cspE* < 0.001, *secG* < 0.005, *RNAI* < 0.05, *osmY* < 0.01, and *dxs* < 0.01) (E) Sequence chromatogram of *osmY* mRNA UTR showing PA-tail addition and the region where PA-tail is added after transcription termination.

(F) 3′-RACE assay of reporter *osmY* mRNA using an engineered oligo-dT primer having a unique sequence at the 3′-end and an *osmY* gene specific forward primer using strains as indicated. See also Figures S1 and S2.

Transgenesis of mammalian PABPN1 stabilizes polyadenylated mRNAs in *E. coli*

qRT-PCR analysis demonstrated that expression of PABPN1 increased levels of earlier known polyadenylated transcripts (*lpp*, *secG*, *rpsO*, *cspE*, *trpA*, *osmY*, and *RNAI*) (Mohanty and Kushner, 2011) but not control non-polyadenylated transcript *dxs* (Figure 1D). Strikingly, there was >3- to 8-fold increase in the expression levels of transcripts tested on PABPN1 expression. Introduction of a PA-tail binding mutant (PABP-Y175A) compromised the stabilization of mRNAs studied (Figure 1D). Consistently, expression levels of the same transcripts were also enhanced on *pcnB* mutation (Figure 1D). We also confirmed polyadenylation of one of the transcript (*osmY*) by 3′-RACE assay followed by 3′-end PA-tail sequencing (Figures 1E and 1F). 3′-RACE assay also showed an increased level of polyadenylated *osmY* transcript and a concomitantly higher total *osmY* mRNA level on PABPN1 expression (Figures 1D, F, S1C). While *pcnB* mutation resulted in the loss of 3′-RACE product, it still augmented the expression level of *osmY* mRNA similar to that of PABPN1 expression (Figures 1D and 1F). Further, measurement of mRNA stability after inhibition of transcription with rifampicin treatment showed around 2- to 4- fold increase in the half-life ($T_{1/2}$) of known polyadenylated mRNAs (*osmY*, *RNAI*) on PABPN1 (but not PABPN1-Y175A mutant) expression (Figure 2A).

Table 1. List of bacterial strains and plasmids employed for the study

Strain	Genotype
DH5α	F⁻ *endA1 glnV44 thi 1 recA1 relA1 gyrA96 deoR nupG purB20* ϕ80d*lacZ*ΔM15 Δ(*lacZYA-argF*)U169, hsdR17($r_K^-m_K^+$), λ⁻
BL21(DE3)	*E. coli* str. B F⁻ *ompT gal dcm lon hsd*S_B($r_B^-m_B^-$) λ(DE3 [*lacI lacUV5-T7p07 ind1 sam7 nin5*]) [*malB*⁺]$_{K\text{-}12}$(λ^S)
MG1655	K-12 F⁻ λ⁻ *ilvG*⁻ *rfb-50 rph-1*
MG-*pcnB*	MG1655 *ΔpcnB759*::*kan*
MG-*PABP*	MG1655::*PABPN1-bla*
MG-*cspE*	*MG1655 ΔcspE762*::*kan*
MG-*hfq*	*MG1655 Δhfq-722*::*kan*
List of plasmids	
pBAD18	Expression vector, pKK223-3 derivative, arabinose inducible expression, pBR322 origin, ampicillin resistance
pET28a	Expression vector, pBR322 origin, N- and C-terminal His-tag on the expressed protein, kanamycin resistance
pCL1920	Cloning vector, pSC101 origin, spectinomycin resistance
pBAD-*PABP*	Derivative of pBAD18 with cloned mammalian nuclear PABPN1 in the *Eco*RI and *Hind*III sites
pBAD-*hfq*	Derivative of pBAD18; *E.coli hfq* full length cloned using *Eco*RI and *Xho*I sites
pBAD-*cspE*	Derivative of pBAD18 with cloned *E. coli cspE* gene in the *Eco*RI and *Xho*I sites
pET-*PABP*	Derivative of pET28a with mammalian nuclear PABPN1 in the *Nde*I and *Hind*III sites
pET-*hfq*	Derivative of pET28a with cloned *E. coli hfq* gene in the *Eco*RI and *Xho*I sites
pET-*cspE*	Derivative of pET28a with cloned *E. coli cspE* gene in the *Eco*RI and *Xho*I sites
pET-$PABP^M$	Derivative of pET-*PABP* with mutation of Y175A by site directed mutagenesis

Plasmids generated and new strains constructed for the study are indicated.

Similar enhancement in the half-life was also visible in the case of *pcnB* mutation. However, there was no additional induction of half-life or mRNA levels on PABPN1 expression in the *pcnB* mutant background (Figure 2A). Together, these results indicate that PABPN1 stabilizes polyadenylated transcripts in *E. coli*.

We then tested PABPN1 binding to one of the bacterial polyadenylated transcripts *in vitro*. We synthesized a radiolabeled *RNAI* with PA-tail (16 adenosines, *RNAI-*A_{16}) and without PA-tail (non PA-tail, *RNAI-*A_0). Subsequently, in EMSA experiments, we observed purified recombinant PABPN1 binding to the *RNAI-*A_{16} but not to the non PA-tail *RNAI-*A_0 (Figures 2B and S1D). The binding was abolished by introduction of a PA-tail binding mutation on PABPN1 (Y175A) (Figure 2B). RNA immunoprecipitation (RIP) experiment also indicated PABPN1 association on the known polyadenylated transcripts *osmY*, *secG* and *rpsO* mRNAs in the cell (Figure 3I). On the other hand, bacterial adenosine binding protein CspE exhibited little affinity toward *RNAI-*A_{16} or *RNAI-*A_0, whereas Hfq was bound to both the transcripts (Figure S1E–S1G). Moreover, ectopic expression of CspE or Hfq had no effect on the expression levels of known PA-tailed mRNAs (*lpp*, *secG* and *RNAI*) and the plasmid copy number unlike PABPN1 expression (Figure S1H and S2A) (PABP expression and plasmid copy number control is detailed in the following section). Consequentially, *pcnB* mutation but not *cspE* mutation stabilized PA-tailed mRNAs (*rpsO*, *lpp*, *secG*, *RNAI*, *trpA*) (Figure S2B). However, *hfq* mutation showed a moderate enhancement in the mRNA levels (Figure S2B) likely through its effect on PAPI activity as described earlier (Hajnsdorf and Regnier, 2000). These results indicate that known *E. coli* adenosine-binding proteins are functionally distinct from PABPN1 in terms of PA-tailed mRNA metabolism and that PABPN1 binding specifically stabilizes polyadenylated transcripts in *E. coli*.

PABP expression phenocopies *pcnB* mutation, alters plasmid copy number control, and compromises PNPase association

Since polyadenylation is known to regulate colE1-based plasmid replication through *RNAI* transcript stability (Xu et al., 1993), we analyzed plasmid copy number control of colE1-based plasmids after PABPN1

A

Half life ($T_{\frac{1}{2}}$) of select mRNAs (minutes)

Strain	*RNAI*	*osmY*	*dxs*
MG1655	1.5 ± 0.4	2.5 ± 0.6	3.8 ± 0.4
MG-*pcnB*	5.6± 0.32	8.2 ± 0.3	4.2±0.52
MG-*PABP*	6.2± 0.56	5.8 ± 0.2	3.6±0.58
MG-*PABP*^{M}	2.1 ±0.21	2.8 ± 0.4	3.8±0.26
MG-*pcnB -PABP*	5.8 ±0.28	6.8 ± 0.6	3.1 ± 0.8

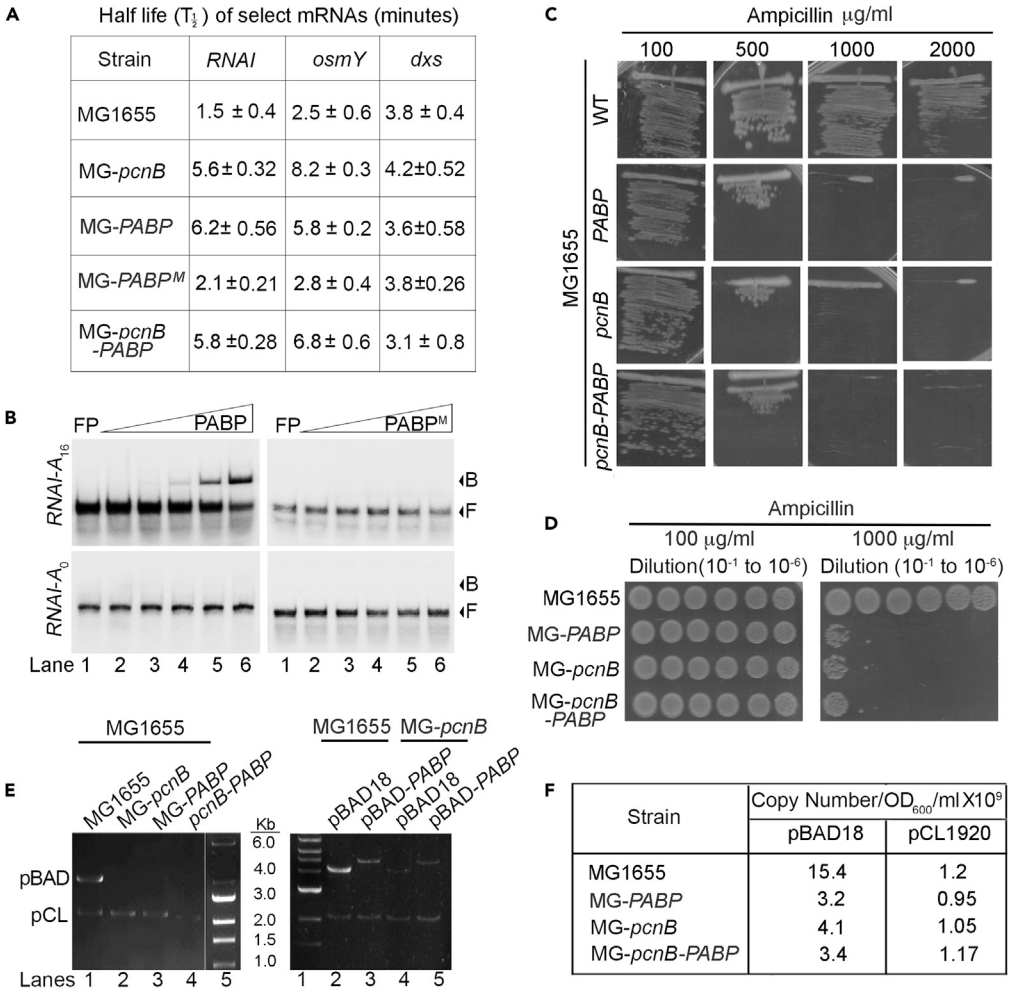

F

Strain	Copy Number/OD_{600}/ml X10^9	
	pBAD18	pCL1920
MG1655	15.4	1.2
MG-*PABP*	3.2	0.95
MG-*pcnB*	4.1	1.05
MG-*pcnB-PABP*	3.4	1.17

Figure 2. Trans-PABPN1 expression phenocopies *pcnB* mutation and alters plasmid copy number control

(A) Half-life ($T_{1/2}$) measurement of cellular polyadenylated transcripts, *RNAI* and *osmY*, and a non-polyadenylated control transcript, *dxs* after inhibition of transcription with rifampicin from various strains as indicated. $T_{1/2}$ is expressed in minutes (min). Data are mean ± SEM of n = 3 independent experiments.

(B) RNA EMSA experiments carried out with *in vitro* transcribed radiolabeled *RNAI* transcript with a PA-tail (*RNAI-*A_{16}) and no PA-tail (*RNAI-*A_0) in the presence of increasing recombinant His-PABPN1 or PA-tail binding mutant His-PABPN1 Y175A (PABP^{M}) (0–30 nM). *RNAI*-PABPN1 binary complex, B and unbound *RNAI*, F and free *RNAI* probe, FP, are indicated.

(C) Antibiotic sensitivity assay of wild-type MG1655, PABPN1 expressed in MG1655 (MG-*PABP*) or *pcnB* mutant (MG-*pcnB*) and PABPN1 expressed in *pcnB* mutant (*pcnB-PABP*) cells transformed with pBAD18 plasmid and streaked on plates supplemented with increasing ampicillin concentration from 100 to 2000 μg/ml as indicated.

(D) Dilution spotting of various strains as in "C" from 10^{-1} to 10^{-6} dilutions on LB plate supplemented with 100 and 1,000 μg/mL ampicillin as indicated.

(E) Analysis of plasmid content of pBAD18 and control pCL1920 plasmids isolated from various strains as in "C" after digestion with *Nde*I to linearize both plasmids.

(F) Copy numbers of pBAD18 and pCL1920 plasmid DNA per 1 OD_{600}/ml (x10^9) from various strains as in "C" as indicated.

See also Figures S1 and S2.

expression. While MG1655 cells grew till 2000-μg/mL ampicillin, PABPN1 expressed cells but not mutant PABPN1 (Y175A) expressed cells were sensitive at 500-μg/mL ampicillin when transformed with pBAD18 plasmid (Figure 2C). Control *pcnB* mutant cells also showed sensitivity at 500-μg/mL ampicillin indicating a decrease in the plasmid copy number on PABPN1 expression or *pcnB* mutation. Similar sensitivity was also observed in dilution plating of the same strains at 500 and 1000-μg/mL ampicillin (Figures 2D and S2C). Subsequently, pBAD18 plasmid content was reduced in control *pcnB* mutant and PABPN1 expressed

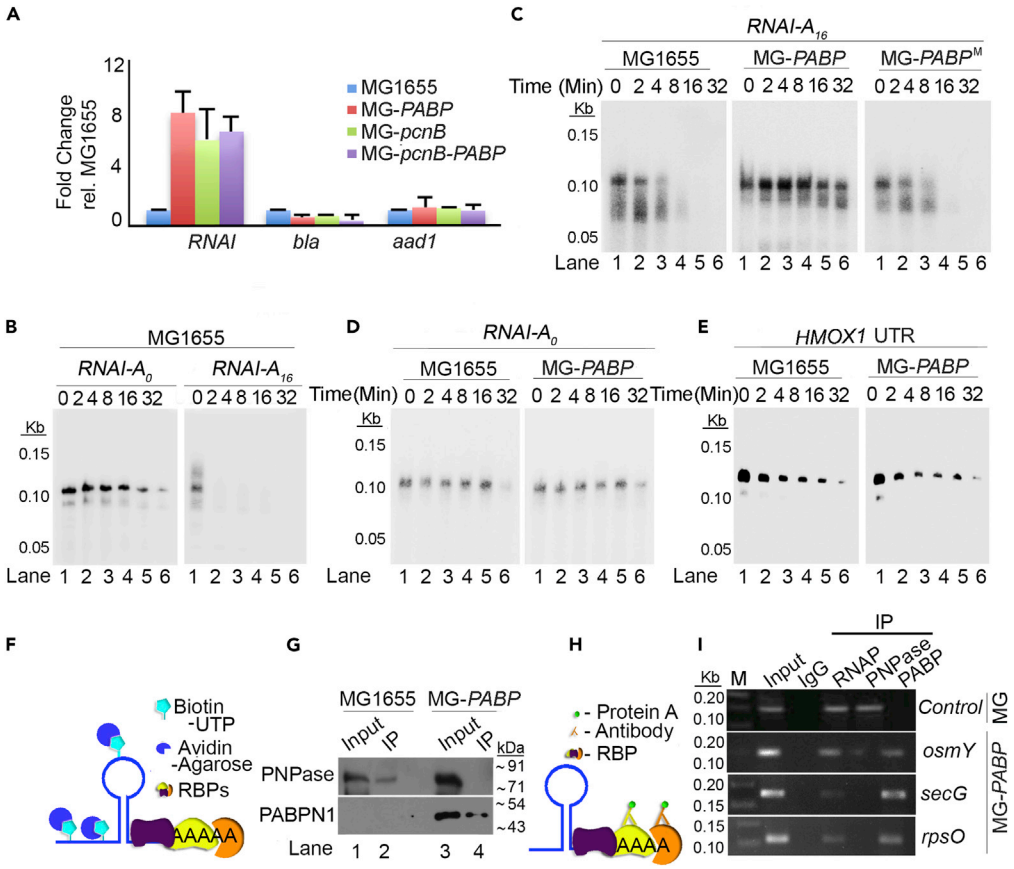

Figure 3. PABPN1 expression protects RNA degradation in the cell lysate and compromises PNPase association

(A) qRT-PCR analysis of *RNAI* transcript, and plasmid borne *bla* gene (encoding ampicillin resistance) and *aad1* gene (encoding spectinomycin resistance) genes from cultures at 1 OD_{600} of various strains as indicated (p values, *RNAI* < 0.05, *bla* < 0.03, and *aad1*<0.001).

(B) Nuclease protection assay of radiolabeled *RNAI-A*$_0$ and *RNA-A*$_{16}$ transcripts incubated with active MG1655 cell extracts (10 μg total protein equivalent) for various time points from 0 to 32 min as indicated.

(C–E) (C) Nuclease protection assay of radiolabeled *RNAI-A*$_{16}$ transcript incubated with active cell extracts (10 μg total protein equivalent) prepared from MG1655, MG-*PABP*, MG-*PABP*^{M} cells for increasing time points from 0 to 32 min (D) Nuclease protection assay of radiolabeled *RNAI-A*$_0$ transcript incubated with active cell extracts (10 μg total protein equivalent) prepared from MG1655 and MG-*PABP* as in b (E) Nuclease protection assay using a non-specific control RNA (mammalian *heme oxygenase 1* (*HMOX1*) UTR RNA fragments of 120-nucleotide length) with MG1655 and PABPN1 expressing (MG-*PABP*) cell lysates as indicated.

(F and G) (F) Schematics of biotin pull-down experiment with a biotin labeled PA-tailed *RNAI-A*$_{16}$ transcript from cell lysates using avidin-coated agarose beads to analyze associated RNA binding proteins (G) Biotin pull-down experiment of *RNAI-A*$_{16}$ incubated with cell lysates from MG1655 and PABPN1 expressed (MG-*PABP*) cells followed by detection of the associated PNPase or PABPN1 proteins by Western blot analysis. Input represents 10% total protein equivalent of the IP samples.

(H and I) (H) Schematics of RIP experiment for PA-tailed RNAs with PNPase, PABPN1, control RNAP and non-specific IgG antibody (I) RIP analysis of PA-tailed mRNA (*osmY*, *secG* and *rpsO*) association with PNPase and PABPN1 from MG1655 cells (control) and PABPN1 expressing (MG-*PABP*) cells. Control RNAP and non-specific IgG is indicated. Input = 10% of the total RNA used for IP.

See also Figures S2 and S3.

(both chromosomally expressed and plasmid expressed) cells with no effect on control *RNAI*-independent plasmid pCL1920 (Figures 2E and S2D). There was ~4-fold reduction in the copy number per OD_{600} per ml of pBAD18 plasmid on *pcnB* mutation and PABPN1 expression (Figure 2F). Consistently, there was increased stability of *RNAI* transcript in PABPN1-expressed cells and *pcnB* mutant cells with no effect on control *bla* expression from pBAD18 or *aad1* mRNA expression from pCL1920 plasmid (Figure 3A). These

results indicate that PABPN1 expression phenocopies *pcnB* mutation and that PABPN1 expression alters plasmid copy number.

To further confirm the stabilization of polyadenylated *RNAI*, we employed *in vitro* transcribed radiolabeled *RNAI-A*$_{16}$ and *RNAI-A*$_0$ transcripts and tested in active MG1655 cell lysate in the presence and absence of PABPN1 expression. As expected, *RNAI-A*$_{16}$ was degraded more rapidly than *RNAI-A*$_0$ in active cell lysate (Figure 3B). We also observed stabilization of *RNAI-A*$_{16}$ but not *RNAI-A*$_0$ in the presence of PABPN1 expression (Figures 3C and 3D). Strikingly, *RNAI-A*$_{16}$ that was degraded after ~2 min in active cell lysate was stabilized by PABPN1 but not mutant PABPN1-Y175A expression (Figure 3C). However, *RNAI-A*$_0$ decay was not affected by PABPN1 expression (Figure 3D). A control mammalian heme oxygenase 1 (*HMOX1*) UTR RNA was degraded alike in both MG1655 and PABPN1 expressed cell lysates (Figure 3E) indicating similar ribonuclease activities of the lysates and the degradation of mRNA. We also observed increased stabilization of *RNAI-A*$_{16}$ in the presence of increasing amounts of recombinant PABPN1 (Figure S2E). To further understand how PABPN1 binding of the PA-tail stabilizes polyadenylated mRNAs in *E. coli*, we pulled down proteins bound on an *in vitro* transcribed biotinylated *RNAI-A*$_{16}$ from cell-extracts of wild type MG1655 and PABPN1 expressed cells and analyzed for the 3′-exonuclease PNPase association (Figures 3F and 3G). We detected PNPase on *RNAI-A*$_{16}$ transcript from wild type cell lysate (Figure 3G). However, PNPase was not detected on *RNAI-A*$_{16}$ from the PABPN1 expressed cell lysate (Figure 3G). Consistently, RIP experiments showed PNPase association with polyadenylated transcripts (*secG*, *osmY*, and *rpsO*) in MG1655 but not in PABPN1 expressed cells (Figures 3H and 3I). Control RNA polymerase (RNAP) was detected on all the transcripts in both cell types. However, PABPN1 was specifically detected on transcripts from the PABPN1 expressed cells and not from the wild type cell lysate (Figure 3I). Together these results indicate that PABPN1 expression compromises PNPase-mediated 3′-exonucleolytic degradation of polyadenylated mRNAs.

PABPN1 expression alters global landscape of mRNA polyadenylation in *E. coli*

Since PABPN1 expression stabilizes known polyadenylated mRNAs in *E. coli*, we carried out genome-wide RNA-Seq analysis of wild-type and PABPN1 expressed (both plasmid-based and chromosomally expressed) MG1655 cells to assess the extent of mRNA polyadenylation in the cell. Of approximately 4,200 protein coding mRNAs in *E. coli* (Serres et al., 2001), we detected more than 3,800 mRNAs (~90% of the total genes) in our RNA-Seq analysis (Figures 4A and 4B). Of these transcripts, we observed approximately 700 mRNAs upregulated on both chromosomal-based PABPN1 expression and plasmid-based PABPN1 expression (Figures 4A and 4B). A list of mRNAs with altered expression from both plasmid and chromosomal PABPN1 expression is shown in Table S1. More than 75% of the upregulated genes were common between the plasmid-based and chromosomal PABPN1 expressed cells (Figure 4C). A list of commonly upregulated mRNAs is shown in Table S2. We then validated 10 genes (*aidB*, *aldB*, *bsmA*, *clpA*, *dsdA*, *osmY*, *otsA*, *uspA*, *uspC*, *uspE*, and *wrbA*) from our RNA-Seq by quantitative real-time PCR (qRT-PCR) analysis (Figure 4D) and 2 mRNAs (*osmY* and *clpA*) by 3′-RACE assay (Figure S3A). We observed up regulation of these mRNAs on PABPN1 expression or *pcnB* mutation in qRT-PCR analysis (Figure 4D). There was similar induction in the 3′-RACE product on PABPN1 expression that was diminished on *pcnB* mutation (Figure S3A).

Further, to validate the induced polyadenylated mRNA level on PABPN1 expression in the cell observed in 3′-RACE, we isolated total cellular PA-plus RNA and analyzed polyadenylated mRNAs by a 3′-end G-I tailing coupled PA-tail assay (Figure S2F) (Kusov et al., 2001; Patil et al., 2014). Here, a short stretch of guanosine and inosine (G-I) nucleotides were added on the *in vivo* isolated PA-plus RNA using yeast PAP (Kusov et al., 2001). Specific mRNAs were further amplified using a reverse primer specific to the added G-I tail and a gene-specific forward primer as in the case of 3′-RACE assay, or by qRT-PCR analysis using the similar primers for quantification (Figure S2F). We consistently observed increased polyadenylated mRNA level (*lpp*, *secG*, *rpsO*, *cspE*, *uspA*, *uspE*, *wrbA*, *rmf*, *cspD*, *and osmY*) in the presence of PABPN1 expression in the cell while non-polyadenylated control *dxs* was negligibly detected in both MG1655 and MG-*PABP* cells (Figure S3B). Similar inductions in the expression levels of these mRNAs (*lpp*, *secG*, *rpsO*, *cspE*, *trpA*, *uspA*, *uspC*, *uspE*, *clpA*, *wrbA*, *rmf*, *cspD*, *otsA*, *and osmY*) were also seen in the qRT-PCR analysis of PA-plus mRNAs (Figure S3C). In line with this, we also observed increased levels of known polyadenylated non-coding RNAs including sRNAs (GlmY, SroH, GlmY) and tRNAs (*valV*, *pheU*, *hisR*, *cysT*) (Mohanty et al., 2020) on PABPN1 expression from the PA-plus RNA analysis (Figure S3D and S3E). However, while majority (~90%) of mRNAs were detected in our RNA-Seq, small RNAs (tRNA or sRNA) were minimally

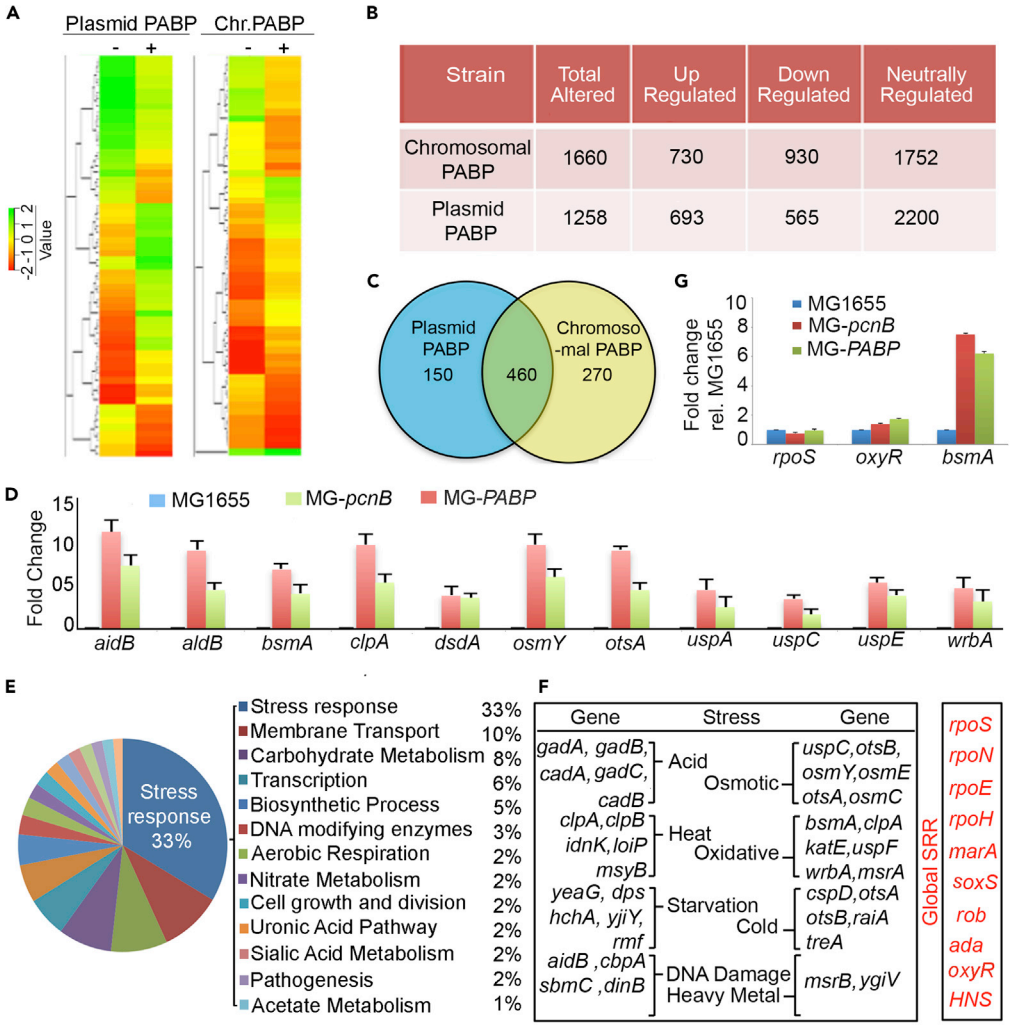

Figure 4. Genome-wide RNA-Seq reveals a new polyadenylation-mediated stress response pathway in *E. coli*

(A) Heatmap showing altered gene expression profile from plasmid-based PABPN1 expressed (plasmid-PABP) and chromosomally expressed PABPN1 (chromosomal PABP) in MG1655 cells compared with the wild-type MG1655 cells.

(B) Table showing number of transcripts altered both upregulated and downregulated on both plasmid PABPN1 expression and chromosomal PABPN1 expression. Complete list of transcripts altered on PABPN1 expression is shown in Table S1.

(C and D) (C) Venn diagram showing upregulated genes overlapped between PABPN1 expressed chromosomally and PABPN1 expressed through plasmid (D) qRT-PCR analysis of 10 select polyadenylated mRNAs from the RNA-Seq data using total RNA isolated from MG1655, *pcnB* mutant (MG-*pcnB*), PABPN1 (MG-*PABP*) expressed cells as indicated (p values for all the genes were <0.001).

(E) Functional pathway analysis of up regulated genes common between PABPN1 expressed chromosomally and PABPN1 expressed through plasmid showing polyadenylated mRNAs involved in multiple cellular functions. Complete list of commonly up regulated mRNAs is shown in Table S2.

(F) List of select genes involved in various stress response pathways from the commonly upregulated genes between PABPN1 expressed chromosomally and PABPN1 expressed through plasmid. Some of the global regulators of stress response that are not affected by PABPN1 expression are shown in the right.

(G) qRT-PCR analysis of *rpoS*, *oxyR* and target gene *bsmA* using total RNA isolated from MG1655, *pcnB* mutant (MG-*pcnB*), PABPN1 (MG-*PABP*) expressed cells as indicated (p values for all the genes were <0.001).

See also Figures S3 and S4.

detected in our RNA-Seq (18 of ~86 total tRNA genes and >85 total sRNAs in *E. coli*). Therefore, we screened total cellular sRNAs and tRNAs using the G-I tailing coupled PA-tail assay described above to assess the effect of PABPN1 trans-expression on these RNAs (Figure S2F). Our screening identified 74 tRNAs and 72 sRNAs, of which RNA levels of only ~19 sRNAs and a majority of ~40 tRNAs were induced on PABPN1 expression. The total list of sRNAs and tRNAs that were stimulated or unchanged on PABPN1 expression from the screening are shown in Table S3. PA-tail assay coupled qRT-PCR screening of 42 select tRNAs and 42 sRNA, along with gel analysis of ~22 select sRNAs and tRNAs from the PA-tail assay is shown in Figures S4A–S4D. Concomitantly, we also observed PABPN1 association with the sRNAs and tRNAs that were induced on PABPN1 expression but not with the unaffected RNAs in the cell (Figures S2F–S2H).

mRNA polyadenylation as a novel stress response mechanism in bacteria

To understand the cellular functions affected by PABPN1 expression, we carried out functional pathway analysis of the upregulated genes on PABPN1 expression (Figure 4E). For our analysis, we considered only those mRNAs that were upregulated in both plasmid-based and chromosomal expression of PABPN1. Our functional analysis revealed involvement of polyadenylation in new cellular functions including membrane transport, different metabolic pathways, pathogenesis, xenobiotic degradation, maintenance of cell wall and membrane integrity, antimicrobial resistance, and aerobic respiration (Figure 4E). Among the PA-tailed mRNAs, the largest fraction (>33%) were those involved in a wide range of stress response pathways including DNA damage, oxidative stress, osmotic stress, heat or cold, nutrient starvation, or biofilm formation (Figures 4E and 4F; Table S4). However, expression of many of the global regulators of stress response including the master regulator gene of stress response *rpoS* (Battesti et al., 2011; Gottesman, 2019; Staroosta et al., 2014) or stress regulator *oxyR* was unaffected (Figure 4G). Whereas, known targets of *rpoS* or *oxyR* were up regulated on PABPN1 trans-expression (Figure 4G). Moreover, tRNA polyadenylation while affects functional tRNA levels, it primarily regulates cellular translation (Mohanty and Kushner, 2012; Mohanty et al., 2012). Furthermore, majority of the stress responsive sRNAs (e.g. OxyS, OmrA, MicC, MicF, GcvB, MgrR, OmrB, RybB, FnrS, ArcZ, DsrA, RprA, and DicF) were unaffected by PABPN1 expression (Table S3) (Gottesman and Storz, 2011; Hobbs et al., 2010; Holmqvist and Wagner, 2017). Together, these results indicate a direct PA-tail stabilization of stress response mRNAs by PABPN1 trans-expression and reveal a new role of global mRNA polyadenylation in general stress response pathway.

PABPN1 expression or *pcnB* mutation alters sensitivity of *E. coli* cells to multiple stresses

To investigate the role of polyadenylation-mediated mRNA turnover in bacterial stress response, we tested stress sensitivity of wild type, *pcnB* mutant, and PABPN1 or PABPN1 (Y175A) PA-tail binding mutant expressed MG1655 cells in six different stress conditions (osmotic stress, oxidative stress, DNA damage/alkylation, acid shock, heat shock and cold shock). While MG1655 cells were viable till 10^{-6} dilutions in control condition, their growth was compromised in all stresses, which was substantially ameliorated by *pcnB* mutation or PABPN1 expression but not by mutant PABP-Y175A expression (Figure 5A). Viable colonies (cfu/mL) were also reduced (~5-10-fold) in wild-type and mutant PABP-Y175A expressed cells with no significant effect in *pcnB* mutant or PABPN1 expressed cells in different stress conditions (Figure 5B). Likewise, in growth curve analysis, all cells reached OD_{600} of ~3.0 under control condition in 12 h, wild-type cells reached OD_{600} only ~1.0 on stress treatment (NaCl, MNNG and acid) (Figured 5C, 5D, and S5A). *pcnB* mutation or PABP expression resulted in a considerable recovery in the growth to ~2.1 OD_{600} under the same stresses (Figures 5C and 5D). Moreover, wild type cells exhibited weak biofilm-forming ability compared to *pcnB* mutant and PABPN1 expressed cells (Figure S5B). Further, we also observed a decrease (~20–~40%) of wild type cell size under high osmolarity as reported earlier (Dai and Zhu, 2018) but no marked changes on the sizes of *pcnB* mutant and PABPN1 expressed cells (Figures 5E and 5F). However, treatment with DNA alkylating agent MNNG resulted in an elongation (~5-fold) of the wild type cells (El-Hajj and Newman, 2015; Uphoff et al., 2016) but did not markedly affect *pcnB* mutant or PABPN1 expressed cells (Figures S5C and S5D). Consistently, qRT-PCR analysis revealed stimulated expression levels of stress response genes (ranging from >10-fold for *bsmA* or *aldB* to 3- to 5-fold for *clpA*, *cspE*, *otsA*, *osmY*, *aidB*, *deoA*) under different stresses (oxidative stress, osmotic stress and alkylation stress) and on PABPN1 expression (Figure S5E). Western blot analysis also showed induced protein levels of stress response proteins (UspF and DsdA) on stress treatment in the presence and absence of *pcnB* mutation or PABPN1 expression (Figure 5G). We also show that PAPI activity is unaffected by PABPN1 expression and PABP and PAPI are functionally distinct (Figures S6A and S6B). Together, our results from PABPN1 transgenesis reveal that 3′-end polyadenylation-mediated mRNA turnover regulates general stress response pathway in *E. coli*.

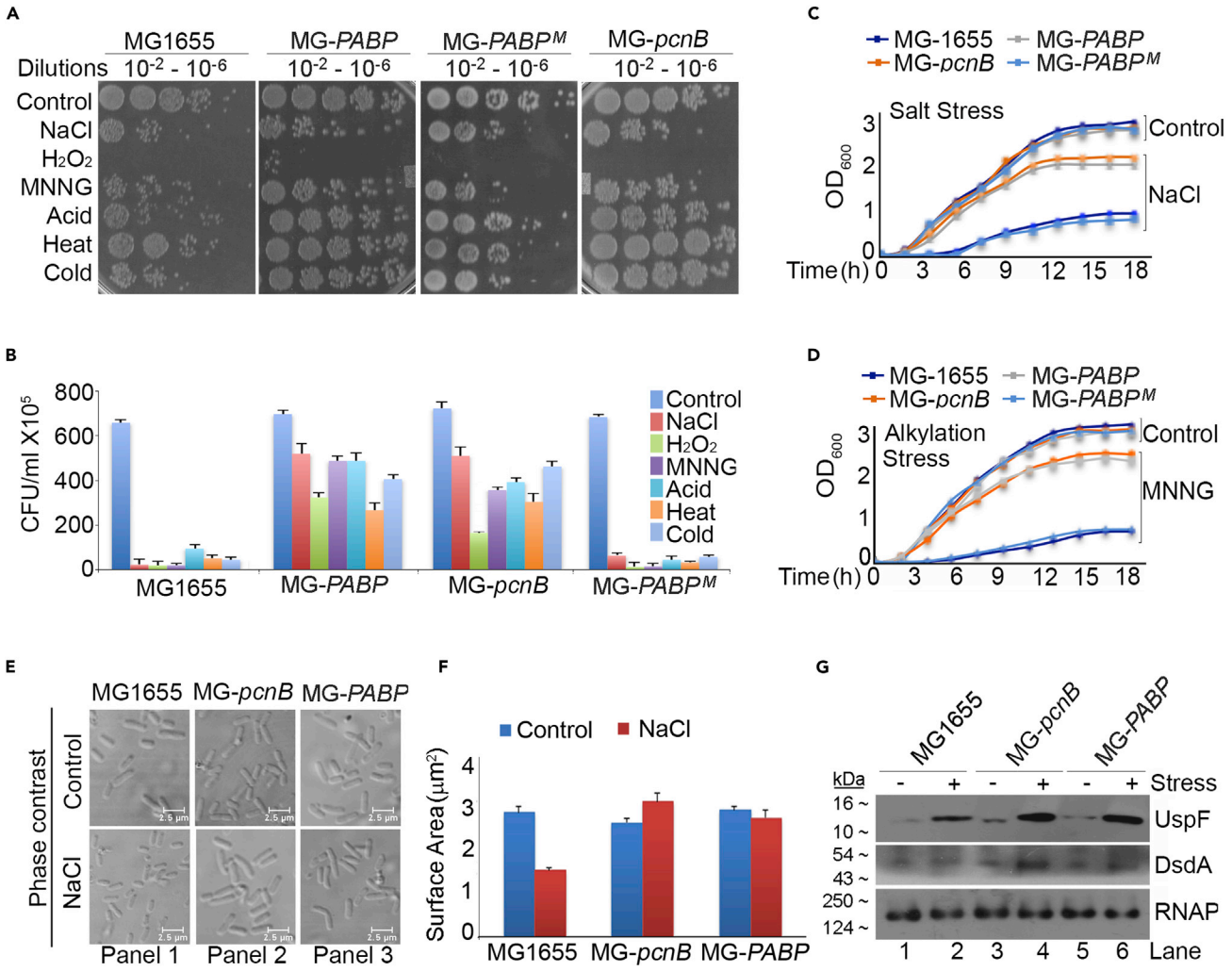

Figure 5. PABPN1 expression or *pcnB* mutation alters sensitivity of *E. coli* cells to multiple stresses

(A) Dilution spotting of MG1655, *pcnB* mutant (MG-*pcnB*), and PABPN1 (MG-*PABP*) or (Y175A) mutant PABPN1 (MG-$PABP^M$) expressed cells after treatment with different stresses at various dilutions from 10^{-2} to 10^{-6} on LB plate as indicated.

(B) Viable colony counting from 10^{-6} diluted cells from stress treated and untreated cultures as in "A" on LB media expressed as colony forming unit (cfu/ml x 10^5) cells (p value <0.005).

(C and D) Growth curve analysis of strains as in "B" strains in the presence and the absence of two select stresses (NaCl and MNNG) as indicated.

(E) Phase contrast image of MG1655, *pcnB* mutant (MG-*pcnB*), and PABPN1 expressed MG-*PABP*) cells after treatment with NaCl and untreated control cells. Scale bar for all images is 2.5 μm as indicated.

(F and G) (F) Quantification of cell surface area (μm^2) of wild-type MG1655, PABPN1 expressed (MG-*PABP*), *pcnB* mutant (MG-*pcnB*) cells in the presence and absence of NaCl treatment as in E. Error bar represents SEM of n = 3 independent experiments (p value <0.001) (G) Western blot analysis of stress response protein UspF and DsdA as indicated. Loading control RNAP is shown below the blot.

See also Figures S5 and S6.

DISCUSSION

Polyadenylation at the structured 3′-end is a key post-transcriptional modification of mRNAs in bacteria that initiates 3′–5′ exonucleolytic degradation, a process critical for mRNA turnover and quality control (Blum et al., 1999; O'Hara et al., 1995). 3′-polyadenylation is primarily carried out by PAPI enzyme in *E. coli* (Cao and Sarkar, 1992). Another protein, the 3′-exonuclease PNPase is also reported to act as a PAP in *E. coli* (Kalapos et al., 1994; Mohanty and Kushner, 2000), yet the exact mechanism how PNPase functions with PAPI for polyadenylation of different cellular transcripts is unclear and is likely dependent on the presence of inorganic phosphates in the cell. However, in mammals, different PAPs (canonical PAPα, PAPγ, and

Star-PAP) exhibit target specificity with distinct niche of mRNA targets for polyadenylation (Li et al., 2017). No such reports for specific target niche selection are available for PAPI or PNPase in *E. coli*. Nevertheless, our genome-wide RNA-Seq analysis after PABPN1 trans-expression shows widespread mRNA polyadenylation in *E. coli*. Moreover, PABPN1 binding alters ramification of 3′-end polyadenylation on mRNA metabolism in *E. coli* that now mimics that of eukaryotes in terms of stabilizing the polyadenylated mRNA. Interestingly, polyadenylation can also mediate RNA decay in eukaryotic cellular organelles such as chloroplast and mitochondria (Schuster and Stern, 2009). While the role of polyadenylation in plant cell chloroplast is similar to that in bacteria, the polyadenylated RNAs in mitochondria are diverse (Levy and Schuster, 2016). Mammalian cell mitochondria harbor both stable polyadenylated mRNAs, and truncated transcripts that are targeted for degradation by polyadenylation(Slomovic et al., 2005). This indicates an intricate evolutionary relationship between polyadenylation and RNA metabolism.

However, unlike in mammals, PABPN1 does not affect PAPI activity or PAPI function (Figure S6A) (Kerwitz et al., 2003). PABPN1 does not exist naturally in *E. coli* and there is also no bacterial counterpart of PABPN1 that specifically protects cellular mRNA PA-tails (Dreyfus and Regnier, 2002). There are two RNA binding proteins, Hfq and CspE that are shown to bind RNAs containing poly-adenosine track in *E. coli*. However, they are functionally different from PABPN1 in PA-tailed RNA metabolism, and their stabilizing effect on PA-tailed mRNA *in vivo* is unclear (Hajnsdorf and Boni, 2012; Hajnsdorf and Regnier, 2000; Mohanty et al., 2004; Phadtare and Inouye, 1999). Thus, this study indicates PABP as a protein at an evolutionary crossroad, emergence of which marks an overturn in the cellular function of polyadenylation on mRNA metabolism (Dreyfus and Regnier, 2002; Hernandez et al., 2010). Our phylogenetic analysis also revealed absence of PABP but presence of PA-tail in archae- and eu-bacteria, and that the PA-tail-mediated mRNA stabilization appeared only in eukaryotes in parallel with the emergence of PABP (Figure S6B).

We have successfully expressed a functional mammalian PABPN1 in *E. coli*, and that PABPN1 binding stabilizes polyadenylated transcripts such as *osmY*. While eukaryotic transgene expression in bacteria is a widely employed approach, trans-expression of eukaryotic proteins functional in bacteria that alters bacterial physiology is still limited (Ostermeier et al., 1996). Our study shows a transgenesis that modifies bacterial physiology and gene expression program including that of stress response, membrane transport, metabolite degradation, and biosynthesis pathways. In addition to the laboratory *E. coli* K-12 strain, the role of polyadenylation in mediating stress response will have ramifications to pathogenic *E. coli* strains and other gram negative pathogens that have PAPI in the cell (Adilakshmi et al., 2000; Hayashi et al., 2001; Saravanamuthu et al., 2004; Welch et al., 2002). Such bacterial pathogens use different mechanisms to adapt and tolerate severe intracellular stress to survive in a host (Fang et al., 2016). Polyadenylation can be one such mechanism that is used by bacterial pathogens. (Our preliminary work also suggest role of polyadenylation in infection and intracellular survival). Similar transgenesis approach can also be used for genetic and metabolic engineering in *E. coli* to modulate biosynthetic pathways to facilitate industrial production of secondary metabolites (Pontrelli et al., 2018). This study unveils a new approach employing functional alien trans-gene expression in bacteria and altering the physiology for industrial and medical applications – a progressive step in applied bacteriology.

Our study shows that polyadenylation-mediated mRNA turnover acts as a general stress response mechanism in *E. coli* and that PABPN1 expression stabilizes stress response mRNAs. Nevertheless, majority of the stress-related regulatory RNAs such as sRNAs are unaffected by PABPN1 expression indicating that PABPN1 primarily stabilizes stress response mRNAs directly through PA-tail binding. We have also confirmed this direct effect of PABPN1 on target PA-tail mRNAs using PABPN1 PA-tail binding mutants. Interestingly, 3′-polyadenylation does not change expression of many of the global regulators of stress response including *rpoS* gene expression. This indicates that the polyadenylation-mediated pathway is a new and an additional mechanism of stress response. However, it is likely to act cooperatively with the transcriptional- and/or small molecule ppGppp-mediated pathways to generate rapid production of effector stress response proteins (Battesti et al., 2011; Gottesman, 2019). Control of mRNA turnover by polyadenylation will prevent futile cycle of transcriptional stimulation that is countered by degradation pathway during stress. In addition, mRNA turnover rate determines the steady state level of an mRNA in the cell affecting its cellular availability for translation (Nouaille et al., 2017). Our study also reveals that mRNA stabilization during stress induces protein expression of stress response regulators in *E. coli*.

Limitations of the study

The polyadenylation mediated general stress response pathway identified in the study may be limited to the bacterial system and may not directly apply to stress response in mammalian or human cells. Moreover, the industrial and medical applications of the metabolic engineering deduced from this study require validation with appropriate model organisms. Understanding the role of mRNA turnover through polyadenylation needs further investigation in pathogenic bacterial strains to understand its role in bacterial pathogenesis.

STAR★METHODS

Detailed methods are provided in the online version of this paper and include the following:

- KEY RESOURCES TABLE
- RESOURCE AVAILABILITY
  - Lead contact
  - Materials availability
  - Data and code availability
- EXPERIMENTAL MODEL AND SUBJECT DETAILS
- METHOD DETAILS
  - Induction of stress response
  - DNA constructs
  - Protein purification
  - Generation of chromosomal insertion
  - Antibiotic sensitivity assay and plasmid copy number analysis
  - Immunoblotting
  - RNA immunoprecipitation
  - Immunofluorescence and imaging
  - Crystal violet assay for biofilm formation
  - Biotinylation pull-down
  - Quantitative real time PCR (qRT-PCR) and half-life measurement
  - 3′-RACE assay
  - *In vitro* polyadenylation assay
  - *In vitro* RNA synthesis, EMSA and nuclease protection assay
  - Genome wide RNA-Seq analysis
  - PolyA+ RNA isolation and PA-tail assay screening
  - Phylogenetic analysis
- QUANTIFICATION AND STATISTICAL ANALYSIS

SUPPLEMENTAL INFORMATION

Supplemental information can be found online at https://doi.org/10.1016/j.isci.2021.103119.

ACKNOWLEDGMENT

We thank Fiona Ukken (University of Wisconsin-Madison, USA) and RSL lab members for carefully reading the manuscript. Various mutant strains (*pcnB*, *hfq, and cspE*) were kind gift from Dr. J. Gowrishankar, Center for DNA Fingerprinting and Diagnostics, Hyderabad. This work was supported by grants from the Department of Biotechnology (BT/PR15554/BRB/101464/2015) and Swarnajayanti Fellowship from the Department of Science and Technology (DST/SJF/LSA-03/2018-19), Government of India to RSL, Indian Council of Medical Research (ICMR) research fellowship to NF.

AUTHOR CONTRIBUTIONS

N.F. planned and carried out all experiments and R.S.L. analyzed and interpreted the experimental data, as well as conceptualized and wrote the paper.

DECLARATION OF INTERESTS

None declared.

Received: February 16, 2021
Revised: April 23, 2021
Accepted: September 9, 2021
Published: October 22, 2021

REFERENCES

Adilakshmi, T., Ayling, P.D., and Ratledge, C. (2000). Polyadenylylation in mycobacteria: evidence for oligo(dT)-primed cDNA synthesis. Microbiology (Reading) *146* (Pt 3), 633–638. https://doi.org/10.1099/00221287-146-3-633.

Aiso, T., Yoshida, H., Wada, A., and Ohki, R. (2005). Modulation of mRNA stability participates in stationary-phase-specific expression of ribosome modulation factor. J. Bacteriol. *187*, 1951–1958. https://doi.org/10.1128/JB.187.6.1951-1958.2005.

Anupama, K., Leela, J.K., and Gowrishankar, J. (2011). Two pathways for RNase E action in Escherichia coli in vivo and bypass of its essentiality in mutants defective for Rho-dependent transcription termination. Mol. Microbiol. *82*, 1330–1348. https://doi.org/10.1111/j.1365-2958.2011.07895.x.

Bardwell, V.J., Zarkower, D., Edmonds, M., and Wickens, M. (1990). The enzyme that adds poly(A) to mRNAs is a classical poly(A) polymerase. Mol. Cell Biol. *10*, 846–849.

Battesti, A., Majdalani, N., and Gottesman, S. (2011). The RpoS-mediated general stress response in Escherichia coli. Annu. Rev. Microbiol. *65*, 189–213.

Belasco, J.G. (2010). All things must pass: contrasts and commonalities in eukaryotic and bacterial mRNA decay. Nat. Rev. Mol. Cell Biol. *11*, 467–478. https://doi.org/10.1038/nrm2917.

Bernstein, P., and Ross, J. (1989). Poly (A), poly (A) binding protein and the regulation of mRNA stability. Trends Biochem. Sci. *14*, 373–377.

Binns, N., and Masters, M. (2002). Expression of the Escherichia coli pcnB gene is translationally limited using an inefficient start codon: a second chromosomal example of translation initiated at AUU. Mol. Microbiol. *44*, 1287–1298.

Blum, E., Carpousis, A.J., and Higgins, C.F. (1999). Polyadenylation promotes degradation of 3′-structured RNA by theEscherichia coli mRNA degradosome in vitro. J. Biol. Chem. *274*, 4009–4016.

Boutet, S.C., Cheung, T.H., Quach, N.L., Liu, L., Prescott, S.L., Edalati, A., Iori, K., and Rando, T.A. (2012). Alternative polyadenylation mediates microRNA regulation of muscle stem cell function. Cell Stem Cell *10*, 327–336. https://doi.org/10.1016/j.stem.2012.01.017.

Boyd, D., Weiss, D.S., Chen, J.C., and Beckwith, J. (2000). Towards single-copy gene expression systems making gene cloning physiologically relevant: lambda InCh, a simple Escherichia coli plasmid-chromosome shuttle system. J. Bacteriol. *182*, 842–847.

Cao, G.J., and Sarkar, N. (1992). Identification of the gene for an Escherichia coli poly(A) polymerase. Proc. Natl. Acad. Sci. U S A *89*, 10380–10384. https://doi.org/10.1073/pnas.89.21.10380.

Carabetta, V.J., Silhavy, T.J., and Cristea, I.M. (2010). The response regulator SprE (RssB) is required for maintaining poly (A) polymerase I-degradosome association during stationary phase. J. Bacteriol. *192*, 3713–3721.

Carpousis, A.J. (2007). The RNA degradosome of Escherichia coli: an mRNA-degrading machine assembled on RNase E. Annu. Rev. Microbiol. *61*, 71–87.

Chomczynski, P. (1993). A reagent for the single-step simultaneous isolation of RNA, DNA and proteins from cell and tissue samples. Biotechniques *15*, 536–537.

Dai, X., and Zhu, M. (2018). High osmolarity modulates bacterial cell size through reducing initiation volume in Escherichia coli. mSphere *3*. https://doi.org/10.1128/mSphere.00430-18.

Dreyfus, M., and Regnier, P. (2002). The poly(A) tail of mRNAs: bodyguard in eukaryotes, scavenger in bacteria. Cell *111*, 611–613.

Eckmann, C.R., Rammelt, C., and Wahle, E. (2011). Control of poly(A) tail length. Wiley Interdiscip. Rev. RNA *2*, 348–361. https://doi.org/10.1002/wrna.56.

El-Hajj, Z.W., and Newman, E.B. (2015). How much territory can a single E. coli cell control? Front. Microbiol. *6*. https://doi.org/10.3389/fmicb.2015.00309.

Fang, F.C., Frawley, E.R., Tapscott, T., and Vazquez-Torres, A. (2016). Bacterial stress responses during host infection. Cell Host Microbe *20*, 133–143. https://doi.org/10.1016/j.chom.2016.07.009.

Feng, Y., Huang, H., Liao, J., and Cohen, S.N. (2001). Escherichia coli poly (A)-binding proteins that interact with components of degradosomes or impede RNA decay mediated by polynucleotide phosphorylase and RNase E. J. Biol. Chem. *276*, 31651–31656.

Folichon, M., Arluison, V.r., Pellegrini, O., Huntzinger, E., Régnier, P., and Hajnsdorf, E. (2003). The poly (A) binding protein Hfq protects RNA from RNase E and exoribonucleolytic degradation. Nucleic Acids Res. *31*, 7302–7310.

Glaunsinger, B.A., and Lee, Y.J. (2010). How tails define the ending: divergent roles for polyadenylation in RNA stability and gene expression. RNA Biol. *7*, 13–17. https://doi.org/10.4161/rna.7.1.10255.

Gottesman, S. (2019). Trouble is coming: Signaling pathways that regulate general stress responses in bacteria. J. Biol. Chem. *294*, 11685–11700. https://doi.org/10.1074/jbc.REV119.005593.

Gottesman, S., and Storz, G. (2011). Bacterial small RNA regulators: versatile roles and rapidly evolving variations. Cold Spring Harb Perspect. Biol. *3*. https://doi.org/10.1101/cshperspect.a003798.

Hajnsdorf, E., and Boni, I.V. (2012). Multiple activities of RNA-binding proteins S1 and Hfq. Biochimie *94*, 1544–1553.

Hajnsdorf, E., and Regnier, P. (1999). E. coli RpsO mRNA decay: RNase E processing at the beginning of the coding sequence stimulates poly(A)-dependent degradation of the mRNA. J. Mol. Biol. *286*, 1033–1043. https://doi.org/10.1006/jmbi.1999.2547.

Hajnsdorf, E., and Regnier, P. (2000). Host factor Hfq of Escherichia coli stimulates elongation of poly(A) tails by poly(A) polymerase I. Proc. Natl. Acad. Sci. U S A *97*, 1501–1505. https://doi.org/10.1073/pnas.040549897.

Hajnsdorf, E., Braun, F., Haugel-Nielsen, J., and Regnier, P. (1995). Polyadenylylation destabilizes the rpsO mRNA of Escherichia coli. Proc. Natl. Acad. Sci. U S A *92*, 3973–3977. https://doi.org/10.1073/pnas.92.9.3973.

Hayashi, T., Makino, K., Ohnishi, M., Kurokawa, K., Ishii, K., Yokoyama, K., Han, C.G., Ohtsubo, E., Nakayama, K., Murata, T., et al. (2001). Complete genome sequence of enterohemorrhagic Escherichia coli O157:H7 and genomic comparison with a laboratory strain K-12. DNA Res. *8*, 11–22. https://doi.org/10.1093/dnares/8.1.11.

He, L., Soderbom, F., Wagner, E.G., Binnie, U., Binns, N., and Masters, M. (1993). PcnB is required for the rapid degradation of RNAI, the antisense RNA that controls the copy number of ColE1-related plasmids. Mol. Microbiol. *9*, 1131–1142. https://doi.org/10.1111/j.1365-2958.1993.tb01243.x.

Hernandez, G., Altmann, M., and Lasko, P. (2010). Origins and evolution of the mechanisms regulating translation initiation in eukaryotes. Trends Biochem. Sci. *35*, 63–73. https://doi.org/10.1016/j.tibs.2009.10.009.

Hobbs, E.C., Astarita, J.L., and Storz, G. (2010). Small RNAs and small proteins involved in resistance to cell envelope stress and acid shock in Escherichia coli: analysis of a bar-coded mutant collection. J. Bacteriol. *192*, 59–67. https://doi.org/10.1128/JB.00873-09.

Holmqvist, E., and Wagner, E.G.H. (2017). Impact of bacterial sRNAs in stress responses. Biochem. Soc. Trans. *45*, 1203–1212. https://doi.org/10.1042/BST20160363.

Iioka, H., Loiselle, D., Haystead, T.A., and Macara, I.G. (2011). Efficient detection of RNA–protein interactions using tethered RNAs. Nucleic Acids Res. *39*, e53.

Jalkanen, A.L., Coleman, S.J., and Wilusz, J. (2014). Determinants and Implications of mRNA Poly (A) Tail Size–Does This Protein Make My Tail Look Big? (Elsevier), pp. 24–32.

Jasiecki, J., and Węgrzyn, G. (2006). Transcription start sites in the promoter region of the Escherichia coli pcnB (plasmid copy number) gene coding for poly (A) polymerase I. Plasmid *55*, 169–172.

Joanny, G., Le Derout, J., Bréchemier-Baey, D., Labas, V., Vinh, J., Régnier, P., and Hajnsdorf, E. (2007). Polyadenylation of a functional mRNA controls gene expression in Escherichia coli. Nucleic Acids Res. *35*, 2494–2502. https://doi.org/10.1093/nar/gkm120.

Kalapos, M.P., Cao, G., Kushner, S.R., and Sarkar, N. (1994). Identification of a second poly (A) polymerase in Escherichia coli. Biochem. Biophys. Res. Commun. *198*, 459–465.

Kerwitz, Y., Kuhn, U., Lilie, H., Knoth, A., Scheuermann, T., Friedrich, H., Schwarz, E., and Wahle, E. (2003). Stimulation of poly(A) polymerase through a direct interaction with the nuclear poly(A) binding protein allosterically regulated by RNA. EMBO J. *22*, 3705–3714.

Kuhn, U., and Wahle, E. (2004). Structure and function of poly(A) binding proteins. Biochim. Biophys. Acta *1678*, 67–84. https://doi.org/10.1016/j.bbaexp.2004.03.008.

Kuhn, U., Nemeth, A., Meyer, S., and Wahle, E. (2003). The RNA binding domains of the nuclear poly(A)-binding protein. J. Biol. Chem. *278*, 16916–16925. https://doi.org/10.1074/jbc.M209886200.

Kusov, Y.Y., Shatirishvili, G., Dzagurov, G., and Gauss-Muller, V. (2001). A new G-tailing method for the determination of the poly(A) tail length applied to hepatitis A virus RNA. Nucleic Acids Res. *29*, E57. https://doi.org/10.1093/nar/29.12.e57.

Laishram, R.S. (2014). Poly(A) polymerase (PAP) diversity in gene expression–star-PAP vs canonical PAP. FEBS Lett. *588*, 2185–2197. https://doi.org/10.1016/j.febslet.2014.05.029.

Lemay, J.F., Lemieux, C., St-Andre, O., and Bachand, F. (2010). Crossing the borders: poly(A)-binding proteins working on both sides of the fence. RNA Biol. *7*, 291–295. https://doi.org/10.4161/rna.7.3.11649.

Levin, P.A. (2002). Light microscopy techniques for bacterial cell biology. Methods Microbiol. *31*, 115–132.

Levy, S., and Schuster, G. (2016). Polyadenylation and degradation of RNA in the mitochondria. Biochem. Soc. Trans. *44*, 1475–1482. https://doi.org/10.1042/BST20160126.

Li, Z., Pandit, S., and Deutscher, M.P. (1998). Polyadenylation of stable RNA precursors in vivo. Proc. Natl. Acad. Sci. U S A *95*, 12158–12162. https://doi.org/10.1073/pnas.95.21.12158.

Li, W., Li, W., Laishram, R.S., Hoque, M., Ji, Z., Tian, B., and Anderson, R.A. (2017). Distinct regulation of alternative polyadenylation and gene expression by nuclear poly(A) polymerases. Nucleic Acids Res. *45*, 8930–8942. https://doi.org/10.1093/nar/gkx560.

Liu, J., and Parkinson, J.S. (1989). Genetics and sequence analysis of the pcnB locus, an Escherichia coli gene involved in plasmid copy number control. J. Bacteriol. *171*, 1254–1261.

Lopilato, J., Bortner, S., and Beckwith, J. (1986). Mutations in a new chromosomal gene of Escherichia coli K-12, pcnB, reduce plasmid copy number of pBR322 and its derivatives. Mol. Gen. Genet. MGG *205*, 285–290.

Maes, A., Gracia, C., Bréchemier, D., Hamman, P., Chatre, E., Lemelle, L., Bertin, P.N., and Hajnsdorf, E. (2013). Role of polyadenylation in regulation of the flagella cascade and motility in Escherichia coli. Biochimie *95*, 410–418.

Maes, A., Gracia, C., Innocenti, N., Zhang, K., Aurell, E., and Hajnsdorf, E. (2016). Landscape of RNA polyadenylation in E. coli. Nucleic Acids Res. *45*, 2746–2756.

Marin-Bejar, O., and Huarte, M. (2015). RNA pulldown protocol for in vitro detection and identification of RNA-associated proteins. Methods Mol. Biol. *1206*, 87–95. https://doi.org/10.1007/978-1-4939-1369-5_8.

Masters, M., Colloms, M.D., Oliver, I., He, L., Macnaughton, E.J., and Charters, Y. (1993). The pcnB gene of Escherichia coli, which is required for ColE1 copy number maintenance, is dispensable. J. Bacteriol. *175*, 4405–4413.

Mellman, D.L., Gonzales, M.L., Song, C., Barlow, C.A., Wang, P., Kendziorski, C., and Anderson, R.A. (2008). A PtdIns4,5P2-regulated nuclear poly(A) polymerase controls expression of select mRNAs. Nature *451*, 1013–1017. https://doi.org/10.1038/nature06666.

Merritt, J.H., Kadouri, D.E., and O'Toole, G.A. (2005). Growing and analyzing static biofilms. Curr. Protoc. Microbiol. Chapter 1, Unit 1B 1. https://doi.org/10.1002/9780471729259.mc01b01s00.

Mohanty, B.K., and Kushner, S.R. (2000). Polynucleotide phosphorylase functions both as a 3′→ 5′ exonuclease and a poly (A) polymerase in Escherichia coli. Proc. Natl. Acad. Sci. U S A *97*, 11966–11971.

Mohanty, B.K., and Kushner, S.R. (2011). Bacterial/archaeal/organellar polyadenylation. Wiley Interdiscip. Rev. RNA *2*, 256–276.

Mohanty, B.K., and Kushner, S.R. (2012). Deregulation of poly (A) polymerase I in Escherichia coli inhibits protein synthesis and leads to cell death. Nucleic Acids Res. *41*, 1757–1766.

Mohanty, B.K., Maples, V.F., and Kushner, S.R. (2004). The Sm-like protein Hfq regulates polyadenylation dependent mRNA decay in Escherichia coli. Mol. Microbiol. *54*, 905–920.

Mohanty, B.K., Maples, V.F., and Kushner, S.R. (2012). Polyadenylation helps regulate functional tRNA levels in Escherichia coli. Nucleic Acids Res. *40*, 4589–4603.

Mohanty, B.K., Agrawal, A., and Kushner, S.R. (2020). Generation of pre-tRNAs from polycistronic operons is the essential function of RNase P in Escherichia coli. Nucleic Acids Res. *48*, 2564–2578. https://doi.org/10.1093/nar/gkz1188.

Nadratowska-Wesołowska, B., Słomińska-Wojewódzka, M., Łyżeń, R., Węgrzyn, A., Szalewska-Pałasz, A., and Węgrzyn, G. (2010). Transcription regulation of the Escherichia coli pcnB gene coding for poly (A) polymerase I: roles of ppGpp, DksA and sigma factors. Mol. Genet. Genomics *284*, 289–305.

Nouaille, S., Mondeil, S., Finoux, A.-L., Moulis, C., Girbal, L., and Cocaign-Bousquet, M. (2017). The stability of an mRNA is influenced by its concentration: a potential physical mechanism to regulate gene expression. Nucleic Acids Res. *45*, 11711–11724.

O'Hara, E.B., Chekanova, J.A., Ingle, C.A., Kushner, Z.R., Peters, E., and Kushner, S.R. (1995). Polyadenylylation helps regulate mRNA decay in Escherichia coli. Proc. Natl. Acad. Sci. U S A *92*, 1807–1811.

Ostermeier, M., De Sutter, K., and Georgiou, G. (1996). Eukaryotic protein disulfide isomerase complements Escherichia coli dsbA mutants and increases the yield of a heterologous secreted protein with disulfide bonds. J. Biol. Chem. *271*, 10616–10622. https://doi.org/10.1074/jbc.271.18.10616.

Patil, D.P., Bakthavachalu, B., and Schoenberg, D.R. (2014). Poly(A) polymerase-based poly(A) length assay. Methods Mol. Biol. *1125*, 13–23. https://doi.org/10.1007/978-1-62703-971-0_2.

Phadtare, S., and Inouye, M. (1999). Sequence-selective interactions with RNA by CspB, CspC and CspE, members of the CspA family of Escherichia coli. Mol. Microbiol. *33*, 1004–1014.

Pontrelli, S., Chiu, T.Y., Lan, E.I., Chen, F.Y., Chang, P., and Liao, J.C. (2018). Escherichia coli as a host for metabolic engineering. Metab. Eng. *50*, 16–46. https://doi.org/10.1016/j.ymben.2018.04.008.

Reichenbach, B., Maes, A., Kalamorz, F., Hajnsdorf, E., and Görke, B. (2008). The small RNA GlmY acts upstream of the sRNA GlmZ in the activation of glmS expression and is subject to regulation by polyadenylation in Escherichia coli. Nucleic Acids Res. *36*, 2570–2580.

Rojas, E., Theriot, J.A., and Huang, K.C. (2014). Response of Escherichia coli growth rate to osmotic shock. Proc. Natl. Acad. Sci. U S A *111*, 7807–7812.

Saravanamuthu, S.S., von Gotz, F., Salunkhe, P., Chozhavendan, R., Geffers, R., Buer, J., Tummler, B., and Steinmetz, I. (2004). Evidence for polyadenylated mRNA in Pseudomonas aeruginosa. J. Bacteriol. *186*, 7015–7018. https://doi.org/10.1128/JB.186.20.7015-7018.2004.

Sarkar, N. (1997). Polyadenylation of mRNA in prokaryotes. Annu. Rev. Biochem. *66*, 173–197. https://doi.org/10.1146/annurev.biochem.66.1.173.

Schuster, G., and Stern, D. (2009). RNA polyadenylation and decay in mitochondria and chloroplasts. Prog. Mol. Biol. Transl Sci. *85*, 393–422. https://doi.org/10.1016/S0079-6603(08)00810-6.

Serres, M.H., Gopal, S., Nahum, L.A., Liang, P., Gaasterland, T., and Riley, M. (2001). A functional update of the Escherichia coli K-12 genome.

Genome Biol. *2*. RESEARCH0035. https://doi.org/10.1186/gb-2001-2-9-research0035.

Shatkin, A.J., and Manley, J.L. (2000). The ends of the affair: capping and polyadenylation. Nat. Struct. Mol. Biol. *7*, 838.

Sinha, D., Matz, L.M., Cameron, T.A., and De Lay, N.R. (2018). Poly (A) polymerase is required for RyhB sRNA stability and function in Escherichia coli. RNA *24*, 1496–1511.

Slomovic, S., Laufer, D., Geiger, D., and Schuster, G. (2005). Polyadenylation and degradation of human mitochondrial RNA: the prokaryotic past leaves its mark. Mol. Cell Biol. *25*, 6427–6435. https://doi.org/10.1128/MCB.25.15.6427-6435.2005.

Starosta, A.L., Lassak, J., Jung, K., and Wilson, D.N. (2014). The bacterial translation stress response. FEMS Microbiol. Rev. *38*, 1172–1201. https://doi.org/10.1111/1574-6976.12083.

Sudheesh, A., Mohan, N., Francis, N., Laishram, R.S., and Anderson, R.A. (2019). Star-PAP controlled alternative polyadenylation coupled poly (A) tail length regulates protein expression in hypertrophic heart. Nucleic Acids Res. *47*, 10771–10787.

Thomason, L.C., Costantino, N., and Court, D.L. (2007). E. coli genome manipulation by P1 transduction. Curr. Protoc. Mol. Biol. mb0117s79. Chapter 1, Unit 1.17. https://doi.org/10.1002/0471142727.

Trapnell, C., Pachter, L., and Salzberg, S.L. (2009). TopHat: discovering splice junctions with RNA-Seq. Bioinformatics *25*, 1105–1111. https://doi.org/10.1093/bioinformatics/btp120.

Trapnell, C., Williams, B.A., Pertea, G., Mortazavi, A., Kwan, G., van Baren, M.J., Salzberg, S.L., Wold, B.J., and Pachter, L. (2010). Transcript assembly and quantification by RNA-Seq reveals unannotated transcripts and isoform switching during cell differentiation. Nat. Biotechnol. *28*, 511–515. https://doi.org/10.1038/nbt.1621.

Uphoff, S., Lord, N.D., Okumus, B., Potvin-Trottier, L., Sherratt, D.J., and Paulsson, J. (2016). Stochastic activation of a DNA damage response causes cell-to-cell mutation rate variation. Science *351*, 1094–1097. https://doi.org/10.1126/science.aac9786.

Welch, R.A., Burland, V., Plunkett, G., 3rd, Redford, P., Roesch, P., Rasko, D., Buckles, E.L., Liou, S.R., Boutin, A., Hackett, J., et al. (2002). Extensive mosaic structure revealed by the complete genome sequence of uropathogenic Escherichia coli. Proc. Natl. Acad. Sci. U S A *99*, 17020–17024. https://doi.org/10.1073/pnas.252529799.

Whelan, J.A., Russell, N.B., and Whelan, M.A. (2003). A method for the absolute quantification of cDNA using real-time PCR. J. Immunological Methods *278*, 261–269.

Xu, F., Lin-Chao, S., and Cohen, S.N. (1993). The Escherichia coli pcnB gene promotes adenylylation of antisense RNAI of ColE1-type plasmids in vivo and degradation of RNAI decay intermediates. Proc. Natl. Acad. Sci. U S A *90*, 6756–6760.

Zheng, D., and Tian, B. (2014). Sizing up the poly(A) tail: insights from deep sequencing. Trends Biochem. Sci. *39*, 255–257. https://doi.org/10.1016/j.tibs.2014.04.002.

STAR★METHODS

KEY RESOURCES TABLE

Reagent or Resource	Source	Identifier
Antibodies		
Mouse monoclonal anti-RNA polymerase β′ 8RB13 antibody	Invitrogen	Cat. No: MA1-25425; RRID: AB_795355
Rabbit monoclonal anti polynucleotide phosphorylase antibody	Bioorbyt	Cat. No: Orb20774 RRID: AB_10936491
Rabbit monoclonal anti-PABPN1 (H-46) antibody	Santacruz	Cat. No: SC-67017 RRID: AB_2156733
Mouse monoclonal β-galactosidase (40-1a)	Santacruz	Cat. No: SC-65670 RRID: AB_831022
Rabbit polyclonal anti-D-serine dehydratase A (DsdA)	Mybiosource	Cat. No: MBS1497575 RRID: NA
Rabbit polyclonal anti-universal stress protein F (UspF)	Mybiosource	Cat. No: MBS7000300 RRID: NA
Bacterial and virus strains		
Please See Table 1		N/A
Chemicals, peptides, and recombinant proteins		
N-Methyl-N′-Nitro-N-Nitrosoguanidine	Sigma	Cat.No: 129941
Isopropyl Thio-β-D-Galactoside	Sigma	Cat.No: 42897
Avidin-Agarose Beads	Thermo Scientific	Cat.No: 20219
biotin16-UTP	Biotium	Cat.No: BU6105H
Rifampicin	Himedia	Cat.No: TC-354-5G
Critical commercial assays		
PA-tail assay kit	Affymetrix	Cat.no: 764551KT
Deposited data		
All sequencing fastq files generated	This Paper	Accession Number: GSE166974
Experimental models: Organisms/strains		
Please See Table 1		N/A
Oligonucleotides		
Please see Table S5		N/A
Recombinant DNA		
Please see Table1		N/A
Software and algorithms		
Image J	NA	https://imagej.nih.gov/ij/download.html

RESOURCE AVAILABILITY

Lead contact

- Further information and requests for resources and reagents should be directed to and will be fulfilled by the Lead Contact, Rakesh S. Laishram (E mail: laishram@rgcb.res.in).

Materials availability

- Plasmids and strains generated in this study are available from the lead contact on request. This study did not generate new unique reagents.

Data and code availability

- The data discussed in this publication have been deposited in NCBI's Gene Expression Omnibus and are accessible through GEO datasets with GEO Series accession number GEO: GSE166974. Accession numbers are listed in the key resources table.
- Any additional information required to reanalyze the data reported in this paper is available from the lead contact upon request.

EXPERIMENTAL MODEL AND SUBJECT DETAILS

All experiments were carried out in *E. coli* K-12 strain MG1655 background. Genotypes of strains employed in the study are shown in Table 1. DH5α strain was used for cloning and plasmid amplification while BL21(DE3) was employed for recombinant protein expression. *pcnB*, *hfq*, *cspE* mutant strains were kind gift from Dr. J. Gowrishankar, CDFD, Hyderabad. Mutants from different bacterial backgrounds were transferred to MG1655 by P1 transduction as described previously (Thomason et al., 2007). All bacterial strains were grown at 37°C in nutrient rich, Luria Bertani or Minimal growth media (containing 0.7% potassium phosphate dibasic, 0.2% potassium phosphate monobasic, 0.1 % ammonium sulfate, 0.05% sodium citrate, 0.01% 0.02% vitamin B1 and 2 mM magnesium sulfate) supplemented with 0.2% glucose or glycerol respectively (Anupama et al., 2011). Arabinose was supplemented in the medium at 0.5% concentration or unless otherwise indicated in the text. Unless otherwise indicated antibiotics were also supplemented at the concentration of 100 μg/ml for ampicillin, 50 μg/ml for Kanamycin, and 50 μg/ml for spectinomycin as described previously (Anupama et al., 2011).

METHOD DETAILS

Induction of stress response

For stress sensitivity assay, cells were grown to approximately $O.D_{600}$ of 0.5 in LB media. To induce different stress response, bacterial culture was treated with 400 mM NaCl (osmotic shock), 5 mM hydrogen peroxide, H_2O_2 (oxidative stress), 25 μg/ml N-methyl-N'-nitro-N-nitrosoguanidine, MNNG (DNA alkylation stress or DNA damage), low pH at 3.0 adjusted with 100% hydrochloric acid, HCl (acid shock), heat shock at 42°C (heat stress), and cold shock at 4°C (cold stress) for one hour each as described earlier (Rojas et al., 2014). After one-hour, cells were serially diluted from 10^{-2} to 10^{-8} in LB and spotted around 5 μl of diluted cultures on LB agar plate and incubated at 37°C. For colony counting, approximately 10^{-6} dilution cells were spread on corresponding selection LB agar plate. Viable colonies were counted and expressed as cfu/ml of cell counts. For growth curve analysis, cells were grown in LB medium containing respective stressors and OD_{600} readings were followed at every hour till the cultures reached stationery phase and graph was plotted with OD_{600} versus time.

DNA constructs

cDNA of eukaryotic PABPN1 was obtained from Origene (PCMV6-AC with cloned PABPN1). Full-length PABPN1 was PCR amplified and cloned at the *Eco*RI and *Hind*III sites of pBAD18 plasmid to generate pBAD18-*PABP*, and at the *Nde*I and *Hind*III sites of pET28a vector to generate pET-*PABP*. PA-tail binding mutations (Y175A) were introduced by site directed mutagenesis as described earlier (Sudheesh et al., 2019). *hfq* and *cspE* were PCR amplified from *E. coli* chromosomal DNA and cloned in *Eco*RI and *Xho*I sites of pET28a (pET-*hfq* and pET-*cspE*) vector respectively for recombinant protein purification. *hfq* and *cspE* were also cloned at the *Eco*RI and *Hind*III sites of pDAB18 plasmid to generate pBAD18-*hfq* and pBAD18-*cspE*. List of primers used for PCR amplification, site directed mutagenesis, inverse PCR and cloning are shown in Table S5.

Protein purification

Recombinant proteins were expressed using pET28 plasmid constructs, overexpressed in BL21(DE3) by inducing with 1 mM isopropyl thio-β-D-galactoside at 18°C. Cells were lysed in ice-cold lysis buffer (20 mM Tris and 200 mM NaCl) and purified by Ni-NTA affinity chromatography as described previously (Sudheesh et al., 2019). The purified proteins were dialyzed in protein storage buffer (20mM Tris-HCl and 100 mM NaCl), concentrated using polyethylene glycol (PEG 20000 mw), snap frozen and stored in -80°C.

Generation of chromosomal insertion

Chromosomal insertion of PABPN1 in the receiver strains MG1655 or *pcnB* mutant (MG1655*ΔpcnB759*::*kan*) strains was carried out using *λ-Inch* technology as described earlier(Boyd et al., 2000). We used the MG1655 bearing pBAD18-*PABP* as donor strain and λ phage integration resulted in the insertion of a region from near *ori* till *bla* gene encompassing the cloned PABP from the pBAD18-*PABP*. Integration occurred in the intergenic region between the *gal* and *bio* operons that flanks the inserted *PABP-bla* gene in the chromosome of receiver strains without disruption of any functional genes generating MG-*PABP* or *pcnB-PABP* strains respectively.

Antibiotic sensitivity assay and plasmid copy number analysis

Antibiotic sensitivity assay (Lopilato et al., 1986) was carried out with wild-type MG1655, and *pcnB* mutant strains transformed with pBAD18 or pBAD18-*PABP* plasmids, and streaked on LB-agar plates in the presence of increasing ampicillin concentration (100 μg/ml to 2000 μg/ml). Alternatively, stable chromosomally inserted strains were transformed with pBAD18 plasmid. To analyze the plasmid content and copy number, above strains were transformed with another an *RNAI* independent non-colE1 plasmid pCL1920. From the cultures collected at different OD_{600} in LB medium, plasmids were isolated by alkaline lysis, digested both pBAD18 and pCL1920 plasmids with *Nde*I, and analyzed on a 1% agarose gel. Copy numbers was calculated by quantifying the amount of plasmids as described earlier (Whelan et al., 2003).

Immunoblotting

For Immunoblotting experiments, cell lysates or IP eluates were resolved on a SDS-PAGE and blotted using specific antibodies on a PVDF membrane as described earlier (Sudheesh et al., 2019). In IP experiments, input was loaded at an amount that is equivalent of 10% of the IP sample.

RNA immunoprecipitation

RIP experiments were carried out after cross-linking total cellular proteins with nucleic acids using 1% formaldehyde in MG1655 and MG-*PABP* cells as described earlier (Sudheesh et al., 2019). The immunoprecipitated samples were eluted and digested with DNaseI, and associated RNA was then detected using one step RT-PCR reaction with gene specific primers. List of primers used for RIP analysis are shown in Table S5.

Immunofluorescence and imaging

Immunostaining was carried out as describe earlier (Levin, 2002). MG1655, MG-*pcnB*, and MG-*PABP* cells were grown upto 0.5 OD_{600} and treated with NaCl and MNNG for one hour. Cells were then harvested at 6000 rpm for 5 minute at 4°C, fixed in ice-cold 80% methanol and 16% paraformaldehyde, followed by permeabilisation with 10 μg/ml of lysozyme. Cells were then mounted on cover slips, pre-treated with 0.1% of poly-L-lysine, blocked with 2% BSA and stained with DAPI. Slides were then imaged on a Nikon A1R Laser scanning confocal microscope as described earlier (Sudheesh et al., 2019). Quantification of the surface are from the phase contrast images was carried out using NIS elements software.

Crystal violet assay for biofilm formation

Cells were grown in 96-well microtiter dishes till OD_{600} = 1. Wells were washed with double distilled water after carefully removing the un-adhered cells. Cells remaining in the wells were then stained with 0.1% crystal violet solution in water for 20 minutes as described previously (Merritt et al., 2005). Unbound dye was then washed off with autoclaved water and the dye bound biofilms were solubilized in 100% DMSO for 20 minutes, and absorbance was measured at 595 nm.

Biotinylation pull-down

For biotinylation pull down, cell lysates were prepared from ~10 ml culture of MG1655 or MG-*PABP* and cells at OD_{600} of ~1.00 were lysed in lysis buffer (10 mM HEPES, pH-7, 200 mM NaCl, 1% Triton-X 100, 10 mM $MgCl_2$, 1 mM DTT and protease inhibitor) as described earlier (Iioka et al., 2011). Briefly, ~30 μg of biotinylated RNA was incubated with 60 μl of pre-washed avidin-agarose beads at 4°C for 1 hr. Agarose beads were washed three times with RNA binding buffer (10 mM Tris HCl, 0.1 M KCl and 10 mM $MgCl_2$), incubated with 5 mg total protein equivalent cell lysates overnight at 4°C. Agarose-beads were collected and washed and proteins were eluted using SDS loading buffer after boiling for 10 minutes at 95°C. Associated proteins were analyzed by Western blotting using specific antibodies.

Quantitative real time PCR (qRT-PCR) and half-life measurement

Bacterial cells were grown in 37°C, harvested at OD_{600} of ~0.6 and total RNA was isolated by trizol method as described earlier (Chomczynski, 1993) and quantified by A_{260} measurement. 2.5 μg of total RNA was used to synthesize first strand cDNA with random hexamers and MMLV reverse transcriptase (Invitrogen). qRT-PCR was performed with gene specific primers and quantified with CFX96 multi-color system using SYBR Green Supermix (Bio-Rad) as described previously (Sudheesh et al., 2019). Single-product amplification was confirmed by melt-curve analysis and primer efficiency was near 100% in all experiments. Quantification is expressed in arbitrary units and target mRNA abundance was normalized to the expression of *dxs* or *rrsA* with the Pfaffle method as described earlier (Sudheesh et al., 2019).

For the half-life measurement of mRNA, cells were treated with 500 μg/ml rifampicin to inhibit transcription and harvested at multiple time points (0 to 20 min) post-rifampicin treatment as described earlier (Sudheesh et al., 2019). RNA was isolated from each cells collected from each time points (0, 1, 2, 4, 6, 8, 12, 16, 24 min). qRT-PCR was carried out and half-life ($T^1/_2$) was measured as described earlier by following the decrease in % mRNA level over time with 0 time point taken as 100% of each gene expression (Sudheesh et al., 2019). List of primers used for qRT-PCR analysis are shown in Table S5.

3′-RACE assay

Total RNA was isolated from *MG1655*, *MG-pcnB* and *MG-PABP* using trizol reagent. For 3′-RACE assay, first strand CDNA was synthesized using MMLV reverse transcriptase and 2-μg of total RNA with Adapter primer at the 5′-end with as described previously (Sudheesh et al., 2019). cDNA was further amplified using genes specific forward primer and AUAP reverse primer. Sequence of Adapter primer, AUAP primer, and gene specific primers are shown in Table S5.

In vitro polyadenylation assay

In-vitro polyadenylation assay was carried out using recombinant His-PAPI on universal A_{45} $(UAGGGA)_5A_{15}$)(Mellman et al., 2008) template with radiolabelled [α-^{32}P]-ATP in a PAP assay buffer (250 mM NaCl, 50 mM Tris-HCl, 10 mM $MgCl_2$ pH 7.9 at 37°C) as described earlier (Mellman et al., 2008). RNA products were analyzed on a 6% urea denaturing poly-acrylamide gel and visualized by phosphor imaging.

In vitro RNA synthesis, EMSA and nuclease protection assay

PA-tailed (*RNAI-*A_{16}) and non(A)-tailed (*RNAI-*A_0) transcripts were prepared by in vitro-transcription using PCR products amplified with a forward primer containing T7 promoter sequence. In the reverse primer 16 Ts were incorporated to generate a short PA-tail of 16 nucleotides whereas for A_0, no overhangs were attached. To prepare the biotin labeled *RNAI*, *in vitro* transcription was carried out with the same PCR product in the presence of biotin16-UTP to obtain a body labeled transcript as described earlier (Marin-Bejar and Huarte, 2015). EMSA experiments were carried out as described earlier in a 20 μl EMSA-binding buffer (10 mM Tris-HCl, pH-7.5, 1 mM EDTA, 50 mM NaCl, 0.5 mM $MgCl_2$, 1 mM DTT) in the presence of 1 μg/ml bovine serum albumin, 50% glycerol with 0.1 nM radiolabeled RNA templates with increasing PABPN1, Hfq and CspE (3 to 30 nM) at room temperature for 30 minutes. The RNA-Protein complex was analyzed on a native polyacrylamide gel and visualized by phosphor imaging.

For nuclease protection assay, active cellular extracts were prepared in a cell lysis buffer containing 50 mM TrisHCl and 10 mM β-mercaptoethanol and digestion of substrate *RNAI-*A_{16} or *RNAI-*A_0 was carried out as described earlier (Feng et al., 2001). ~5 nM of radiolabelled *in vitro* transcribed RNA substrates were incubated with 4 μg equivalent of each active cell lysates for various time points as indicated. The residual RNA was then purified by phenol-chloroform, precipitated and analyzed on a urea-denaturing acrylamide gel and visualized by phosphor imaging.

Genome wide RNA-Seq analysis

RNA extracted from pellets of MG1655, MG-*PABP*, MG-*pcnB* were analyzed for QC using Bioanalyser and Qubit. Library preparation and deep sequencing of each sample was performed at commercially available genomics facility at the Genotypic Technology, Bangalore-India (https://www.genotypic.co.in). 4 μg of QC

passed total RNA was used for ribo-depletion using RiboMinus Bacterial Kit (Invitrogen). Further, 100 ng of Qubit quantified ribo-depleted RNA was taken for Transcriptome library preparation according to Sure Select Strand-Specific RNA Library Prep Kit protocol outlined in "SureSelect Strand-Specific RNA Library Prep for Illumina Multiplexed Sequencing" (Illumina). Briefly, the RNA was fragmented for 4 minutes at 94°C in the presence of divalent cations and first strand cDNA was synthesized. The single stranded cDNA was cleaned up using High Prep (Magbio, Cat # AC-60050). Strand specificity was maintained by the addition of actinomycin D. Second strand cDNA was synthesized and end repaired using Second Strand Synthesis using End Repair mix. The cDNA was cleaned up using High Prep (Magbio, Cat # AC-60050). Adapters were ligated to the cDNA molecules after addition of "A" base. High Prep cleanup was performed post ligation. The library was indexed and enriched for adapter ligated fragments using 10 cycles of PCR. The prepared library was quantified using Qubit and validated for quality by running an aliquot on High Sensitivity Bioanalyzer Chip (Agilent). 150 (75X 2) bp Paired End Sequencing was carried out on Illumina platform to generate 20-25 million PE Reads per sample. Bioinformatics analysis was performed with algorithms for Alignment Statistics, Reference alignment with depth statistics, digital gene expression, and DEseq plot read counts. The raw data generated was checked for the quality with FastQC1 and pre-processed to remove adapter sequences and low quality bases. It was then aligned using Tophat-2.0.133 (Trapnell et al., 2009) to *E. coli* (K-12) (Ensembl https://bacteria.ensembl.org/Escherichia_coli_str_k_12_substr_mg1655_gca_000005845/Info/Index/) reference genome. Transcript assembly was done using Cufflinks-2.2.1 (Trapnell et al., 2010) which assembles transcripts, estimates their abundances, and tests for differential expression and regulation in RNA-Seq samples. Then, using cuffmerge, cufflinks assemblies were combined followed by differential gene expression analysis using "Cuffdiff" to obtain the significant changes in transcript expression (Trapnell et al., 2010). Uniprot knowledge base was used to annotate the genes for Gene Ontology (GO) (Boutet et al., 2012). Differential gene expression studies were carried out between PABPN1 expressed group versus wild type MG1655 samples. Differentially expressed genes were further annotated for the protein name and Gene Ontology and heat map generated as a representation of the expression values (as colors). The raw RNA-Seq data of our study has been deposited in the NCBI GEO sequencing data repository.

PolyA+ RNA isolation and PA-tail assay screening

Bacterial cells were grown in 37°C, harvested at OD_{600} of ~0.6 and total cellular PA-plus RNA was isolated using Oligotex PA-plus RNA isolation kit (Qiagen) as per the manufacturers instruction. Eluted PA-plus RNA was quantified and employed for G-I tailing and cDNA synthesis for downstream 3'-end PA-tail assay (PA-tail assay kit, Affymetrix) as described previously (Kusov et al., 2001; Patil et al., 2014). For G-I addition at the 3'-end, ~500 ng of purified PA-plus RNA was incubated with yeast PAP in the presence of guanosine triphosphate (GTP) and inosine triphosphates (ITP) at 37°C for one hour. First strand cDNA was then synthesized from G-I tailed RNA using G-I tail specific reverse primer. cDNA was then used for both qualitative and quantitative PCR. For PCR amplification a gene specific forward primer (GSP) and a universal reverse primer (URP) specific for the added G-I tail was used. Qualitative PCR was analyzed by agarose gel electrophoresis and quantitative analysis was carried out by real-time qPCR using similar primers and expressed as relative RNA levels. Schematic depicting the PA-tail assay system is shown in Figure S2F. Screening of cellular ~86 tRNAs and ~85 sRNAs was carried out by PA-tail assay using forward primers specific to each tRNA or sRNA and a universal reverse primer specific to the G-I tail addition as described above. Changes in the polyadenylated RNA levels were analyzed qualitatively by PA-tail assay coupled RT-PCR and quantitatively by real-time qPCR.

Phylogenetic analysis

We carried out an exhaustive literature analysis for the occurrence of poly(A) binding proteins, poly(A) polymerase and mRNA stabilization by polyadenylation across various branches of the evolutionary tree. Published literatures, NCBI protein search and protein databases such as pfam were used as reference to mark presence or absence of identified PAPs or PABP protein in organisms across different phyla in the evolutionary tree. We however ignored the hypothetical proteins and un-annotated proteins from the finding. Further, phylogenetic tree was later constructed with the available occurrence with representations from all the domains across all kingdoms.

QUANTIFICATION AND STATISTICAL ANALYSIS

All data were obtained from at least three independent experiments and are represented as mean ± standard error mean, SEM. The statistical significance of the differences in the mean is calculated using ANOVA with statistical significance at a p-value of less than 0.05. All Western blots shows representative of at least from three independent blotting experiments. Quantifications of blots were carried out with Image J software.